INTERNATIONAL METALS REVIEWS

Rolling of rings
W. Johnson and A. G. Mamalis

Physical and chemical nature of cemented carbides
H. E. Exner

INTERNATIONAL METALS REVIEWS

1979 Volume 24 Number 4

International Metals Reviews

1979 Volume 24 Number 4

CONTENTS

INHALTSVERZEICHNIS

137 Ringwalzen *W. Johnson und A. G. Mamalis*

Das Ringwalzen, als Warmverformungsvorgang und als Kalt-verformungspräzisionsvorgang zur Herstellung von kleinen Ringen mit kleinem Profil, ist ein in der Industrie wohl bekanntes Verfahren. Die Verfahren und die mechanischen Vorgänge des Vorganges werden besprochen um den Leser auf die darüber vorhandene Information aufmerksam zu machen.

149 Die physikalischen und chemischen Grundlagen der Hartmetalle

Vom technischen Standpunkt aus zählen die Hartmetalle zu den erfolgreichsten Verbundwerkstoffen. Unter Betonung der werkstoffwissenschaftlichen Gesichtspunkte wird ein Überlick über die physikalischen und chemischen Grundlagen der Komponenten (Übergangsmetallkarbide und Metalle der Eisengruppe) und über ihre Wechselwirkung in den Hartmetallen gegeben. Im Vordergrund stehen dabei die Hartlegierungen, die technische Bedeutung gewonnen haben. Die Kristallstrukturen und

H. E. Exner

die Phasenbeziehungen werden im Detail besprochen. Auch die Wechselwirkung der Komponenten (Benetzung, Restspannungen) und einige Gefügedetails (Größe und Form der Kristalle, Skelettbildung) werden behandelt. Die Kenntnis dieser Grundlagen sind eine notwendige Voraussetzung zum Verständnis der Herstellungsprozesse und der Eigenschaften von Hartmetallen.

TABLE DES MATIERES

137 Laminage des produits annulaires *W. Johnson et A. G. Mamalis*

Le laminage des produits annulaires est bein établi dans l'industrie en tant que procédé de formage à chaud ou à froid pour la production de petits produits annulaires profilés. Les pratiques et les méchaniques du procédé sont passées en revue dans le but d'attirer l'attention sur les reseignements utiles actuellement disponibles les concernant.

149 Nature physique et chimique des carbures frittés *H. E. Exner*

Les carbures frittés sont, d'un point de vue technique, l'un des matériaux composites les plus satisfaisants. Les caractéristiques physiques et chimiques de leurs constituants (carbures de métaux de transition et métaux du groupe du fer) et de leurs interactions dans les métaux durs sont passées en revue en s'occupant particulièrement au point de vue science des matériaux, des compositions présentant un intérêt technique. Les structures cristallines et les relations entre phases sont discutées en détail. De même, l'interaction entre composants (mouillage, contraintes résiduelles) et certains aspects de leur microstructure (taille, contiguité et forme) sont traités. Ces problèmes fondamentaux constituent la base de la compréhension des processus de fabrication et des propriétés des carbures frittés.

Rolling of rings

by W. Johnson and A. G. Mamalis

Ring rolling as a hot-forming process and as a cold-forming precision process for producing small profiled rings is well established in industry. The practices and the mechanics of the process are reviewed with the aim of drawing attention to useful available information about it.

A classification of metal flow processes is to be had by reference to the plane-strain indentation or forging of a block by opposed flat rigid dies as in Fig. 1; the geometry of the various forming processes are related[1] to one another therein and, in particular, the range to which the subject of this paper applies is clearly identified.

Ring rolling is a specialized form of rolling process and its value and virtues do not appear to be as widely appreciated as they should by metal formers. It is not a new method because railway tyres have long been made by this technique.

The production of relatively thin annular parts covers a wide range from mass-produced small components — inner and outer bearing races, for example — to large-dimension rings, such as those for reinforcing pressure vessels. During recent years the process has been increasingly applied in a number of fields owing to its technological advantages when compared with other techniques used for the production of rings, e.g. casting, the bending of profiles and the welding of the ends, and forging. The newer applications are to the manufacture of annular parts for jet engines and for large rings of special alloys for rockets and spacecraft.

The advantages of ring rolling are a much shorter production time, uniform quality because of the induced circumferential grain flow (the benefit is most evident in life improvement conferred on bearing races), close tolerances, and especially the considerable saving in material costs — about 90% of the input weight turns into finished product.

An earlier review of the practices and the mechanics of this process which the present article encompasses may be found in Ref. 2.

Professor W. Johnson is in the Department of Engineering, University of Cambridge, and Dr A. G. Mamalis is presently Humboldt Research Fellow, Lehrstuhl und Institut für Fertigungstechnik und spanende Werkzeugmaschinen, Technische Universität, Hanover, West Germany.

MANUFACTURING PROCESSES AND PRACTICES

Equipment

The first machine for making rings was constructed in England in 1827; it produced shaped bars by bending flat strip into a circular form with the bar ends being welded to form the ring.

Bodmer[3] in 1842 appears to have been the first designer of a ring-rolling mill to produce seamless rings for P. R. Jackson and Co. of Manchester.

The first attempt in Germany was made by Alfred Krupp in 1849 for the purpose of producing railway tyres; he constructed the first ring-rolling mill in 1853—54 and by 1855—56 he had modified it to accommodate two-stage rolling. Several modifications to ring-rolling mills were patented later by Huffam[4] in 1884, Willford[5] in 1891, and Muller[6] in 1896.

A ring-rolling mill which is basically the prototype for the modern mills was constructed by Demag at the beginning of the century; it was furnished with a driven main roll, a thrust roll hydraulically operated, and centring rolls.

Different types of ring-rolling mills have been developed according to the size of the ring being produced. For the large-scale production of small rings, a mechanical four-mandrel mill is used. It consists of a driven roll and four mandrels mounted on a rotating table whose centre is eccentric to the driven roll; the blank is placed over a mandrel and is expanded as the throat depth between the mandrel and the driven roll decreases, see Fig. 2.

Rings of medium or large sizes are produced in a small series or as single parts on hydraulic single-mandrel mills. In the case considered, the ring is formed between an internal undriven mandrel free to rotate, and an external driven roll, see Fig. 3a; reduction in ring wall thickness and, consequently, an increase in its diameter is achieved by moving the mandrel hydraulically towards the main roll. Small centring rolls are used to keep the ring in a central position and to maintain its circularity. Automatic mills are being produced now as single-mandrel hydraulic machines and radial or radial—axial mills where the edge faces of the ring are controlled by a pair of conical, axial rolls operating diametrically opposite the radial rolls which cause the ring to expand, see Figs. 3b and 4.

Recent developments in commercial ring-rolling mills are given mainly (and in detail) by German mill manufacturers, see Refs. 7—14. A
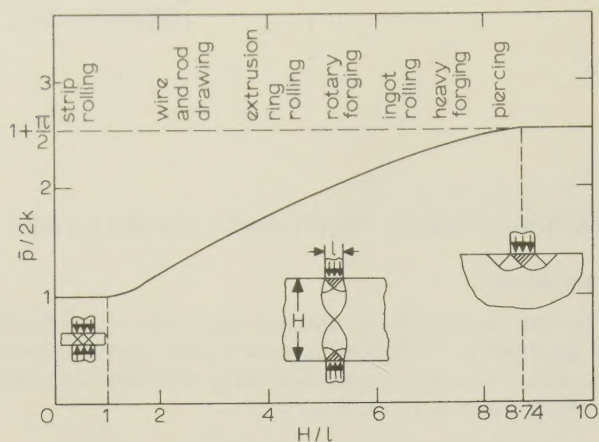
1   **Classification of forming processes**

description of a *vertical* ring-rolling prototype mill, now not in use, is given in Ref. 15. Further details concerning a production line for rings, such as furnaces for heating of the billets, electrical equipment, control, transport, and layout of an industrial plant are reported in Refs. 16—20.

Applications

As stated above, the range of configurations and dimensions which is covered by ring rolling is very wide; typical applications are tyres for railway wheels and cranes, inner and outer races for ball and roller bearings, flanges, gearwheel rims, reinforcing rings for pipes and pressure vessels, and large rings for gas turbines and rockets. Typical cross-sections that can be produced by ring rolling are presented in Fig. 5a. Figure 5b is a rolled ring gear and Fig. 5c is a heavily rolled down, thin copper belt. Figure 5d shows a ring typically malformed owing to insufficient roll load.

Recent developments in ring-rolling applications have been discussed in Ref. 21. In Refs. 22—28 a survey of the wide range of products achieved
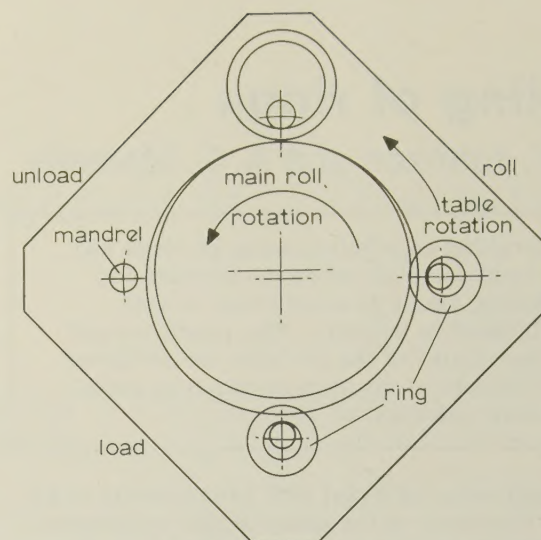
2   **Mechanical 4-mandrel ring-rolling mill (principle)**

by ring rolling and forging is outlined, *see* also Fig. 5a, and the size and shape limitations of rings rolled in industrial practices are given. It is maintained in Ref. 22 that the maximum size of a ring that can be rolled is limited only by the capacity of the available equipment. (Most rolled rings are 30—75 cm in outside diameter, but both smaller and much larger rings are in common use.) The minimum practical size of a rolled ring is limited primarily by roll dimensions and by the amount of rolling required.

The cold rolling of gears, *see* Fig. 5b, is considered, in detail, in Refs. 29 and 30. The cold forming of inner and outer ball-bearing races has also been examined under the title of form rolling,[31,32] *see* Fig. 6; details concerning the manufacture of ball-bearing races are also given by various well known European and Japanese ball- and roller-bearing manufacturers, *see*, for example, Refs. 31—34.
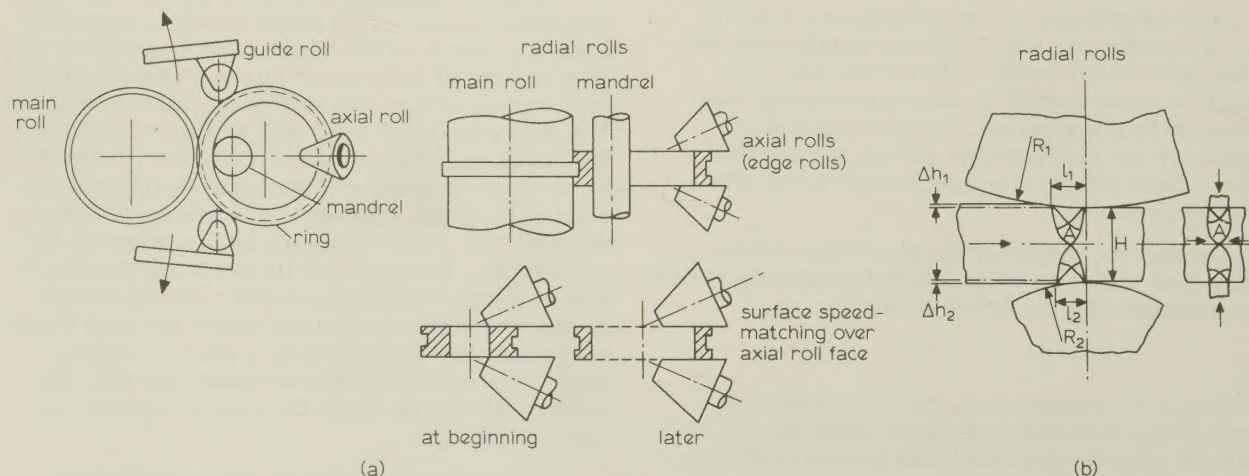
3   *a* hydraulic ring-rolling mill with radial and axial rolls (principle) and *b* assumed field in roll gap and corresponding slip-line field for indentation
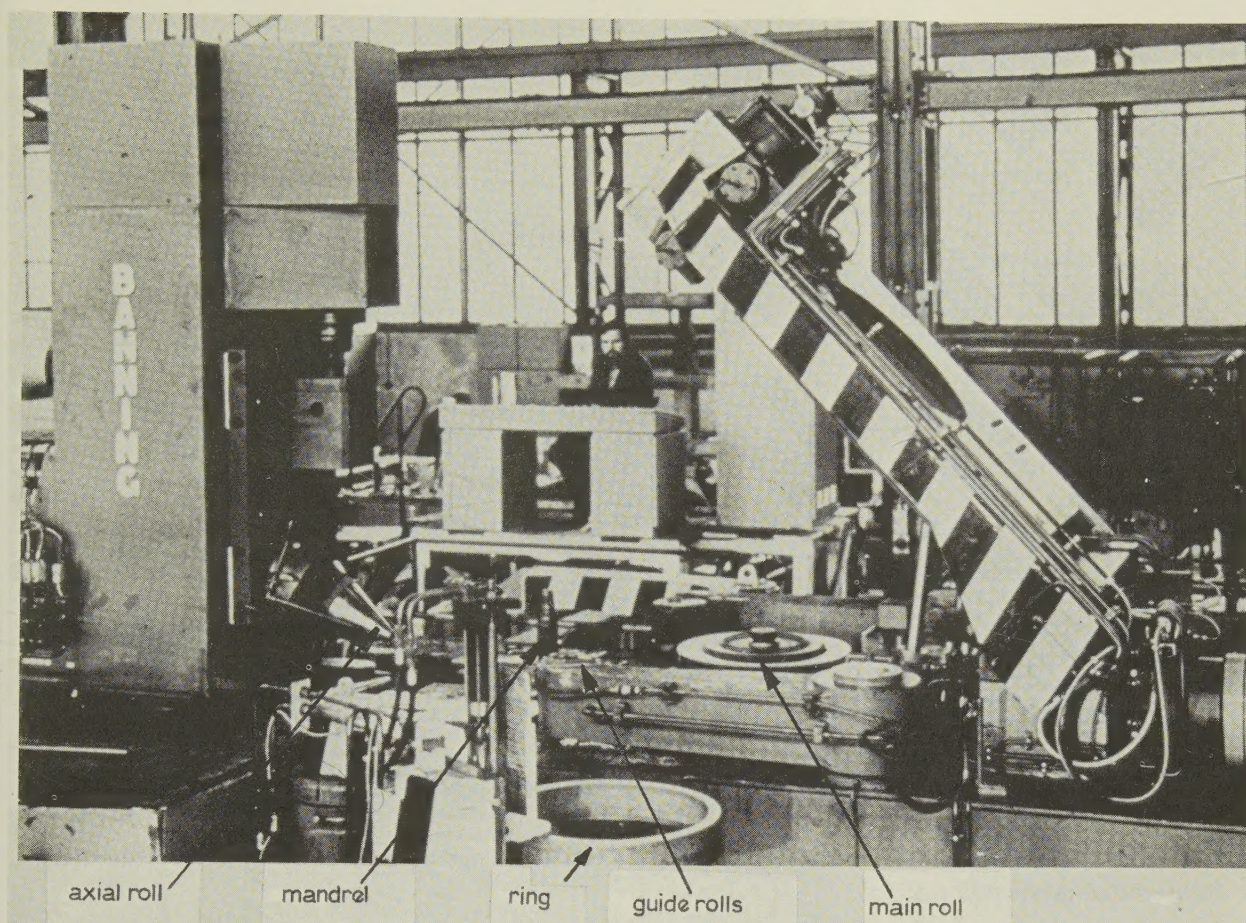
4   General view of a modern hydraulic ring-rolling mill

Configurations can be usefully divided, in general, into three categories:

(i)   rings with a small wall thickness/diameter ratio and (a) a height larger than the wall thickness, e.g. radial roller-bearing races, or (b) a height smaller than the wall thickness, e.g. thrust roller-bearing races

(ii) extremely thin-walled rings of large diameter, e.g. reinforcing rings for pipes and pressure vessels

(iii) thin-wall rings of height about equal to a diameter, e.g. double-row freight-car bearing races.

Railway tyres and solid wheels have long been formed by ring rolling; Lehmann,[35] and especially Shifrin and co-workers[36-38] in the USSR describe this particular kind of manufacturing process, but *see* also Refs. 39 and 40.

Apart from all the applications mentioned above, ring rolling has been used for the production of sections which, because of the requirement for only small quantities or because of the high price of superalloys, are very expensive to produce by extrusion or conventional rolling; the rings are parted off after rolling and straightened. In a similar manner, small quantities of strip and plate can be used to produce thin-walled and large-diameter rings. A production line, engineered by the American company, Grotnes Ltd, which combines ring rolling and current-penetration bar butt welding, and turns flat steel strips into cylinders for making automobile rim blanks for General Motors, is described in Ref. 41. Grotnes Ltd[42] has demonstrated also a machine that produces a profiled ring by cold forming the cross-section of the blank (a hoop of welded bar stock) between two rotating rolls. It is claimed that General Electric (USA) has such a machine in commercial operation making precision profiled rings for their aircraft jet engines.

A method in which a cold metal ring is greatly expanded in radial diameter and simultaneously contoured to a desired cross-sectional shape by successively rolling the ring between selected pairs of roll dies has been patented recently by General Electric in the USA[43] for manufacturing metal rings suitable for use in gas-turbine engines; high accuracy and tolerance, and small production times are claimed.

Also worth mentioning is a recent attempt to apply the ring-rolling process to powder metallurgy. The development of a ring-rolling mill for this purpose in Japan is reported[44] and in the USA
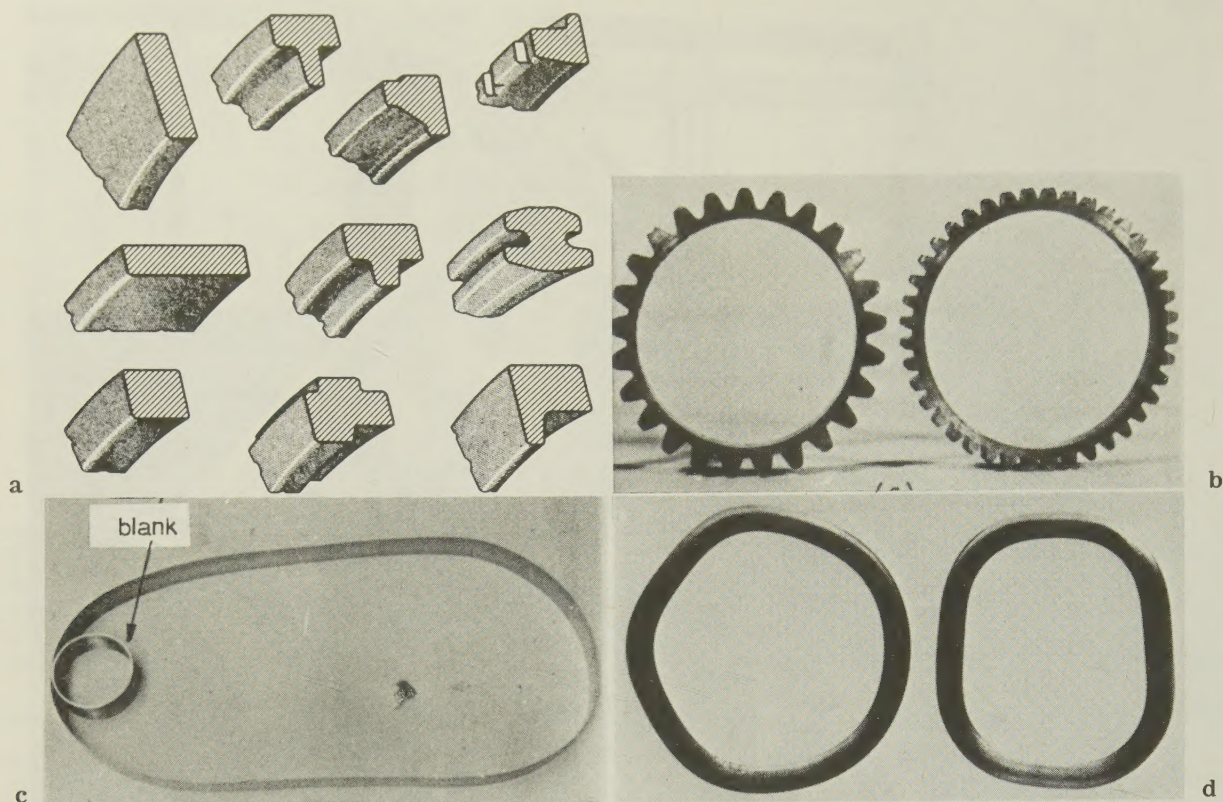
a typical cross-sections; *b* gears; *c* copper belt; *d* distorted rings owing to insufficient rolling load

5   Ring-rolled products

the particle ring-rolling process, called PR^2, was developed.[45] The PR^2 process is a ring-rolling process in which the workpiece is comprised of metal particles encapsulated in a toroid or dough-nut-shaped metal container. During rolling the particles are consolidated and deformed and the workpiece is expanded to form a metal ring of the desired diameter, thickness, and configuration. It is claimed that the process has been completely successful in the fabrication of rings from alumin-ium and nickel powders and that a metallurgical bond has been developed between the material of the container and the consolidated particle mass.

One of the principal advantages of the ring-rolling process is that it saves metal that would be punched out in conventional closed-die forging or machined out in a machining operation. As stated above, it is estimated that in ring rolling about 90% of the input weight is turned into finished product. To emphasize the importance of this forming process a recent statement (1976), repeated here, was to the effect that if the rings of expensive material used in the Rolls-Royce jet engine RB 211 could be formed by ring rolling rather than machining, the price of an engine could be reduced by about $100000.

A comparison of the manufacturing cost of closed-die forging and ring rolling with subsequent machining costs is given in Fig. 7, reproduced from

6   Cold ring rolling of *a* inner and *b* outer ball-bearing races (Formflo)
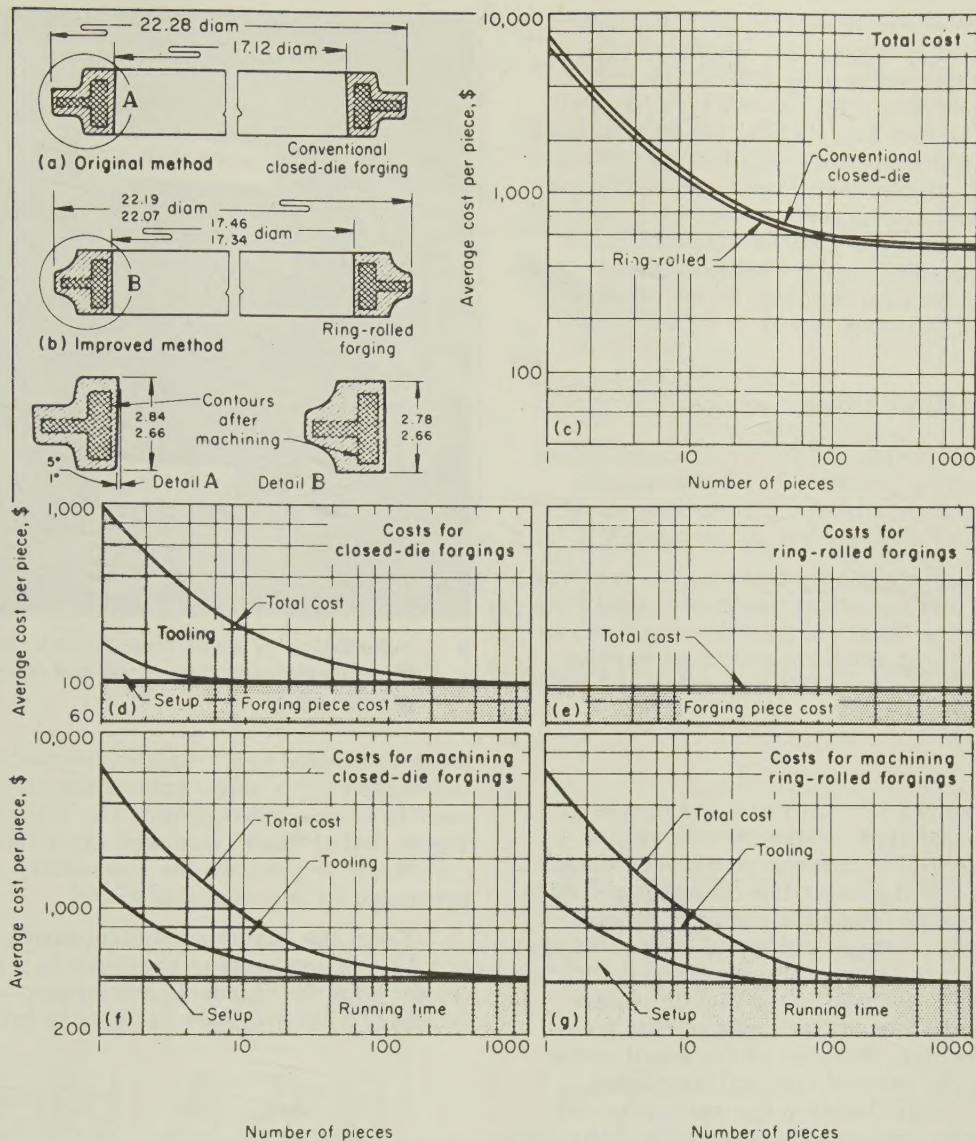
Item	Closed-die forgings	Ring-rolled forgings	Item	Closed-die forgings	Ring-rolled forgings
Manufacturing Details			**Cost Details — Unit One**		
Material	AMS 6260	AMS 6265(a)	**Forging:**		
Forging equipment ...	8000-lb	Ring-rolling	Die cost	$ 800	(b)
	hammer	machine to	Setup cost	70	(b)
	to finish	finish	Forging piece cost	110(c)	$ 96
Forging operations	Pancake	Pancake	Forging cost, unit one	$ 980	$ 96
	and plug	and plug	**Machining:**		
	Punch out	Punch out	Tooling cost	$5000	$5000
	Saddle forge	Ring roll to	Setup cost	1000	1000
	for blocker	contour	Running cost	425	415
	Finish forge		Machining cost, unit one ..	$6425	$6415
Machining operations (both types of forgings)	Lathe turn Shape gear teeth Drill, ream 24 fastener holes Grind gear teeth		Total forging plus machining costs, unit one	$7405	$6511

(a) Composition is the same as AMS 6260, except that the steel is premium quality, consumable electrode, vacuum melted. (b) Because the ring-rolled forging employed available stock tooling, die and setup costs were absorbed by the forging producer; use of facilities and labor are reflected in the forging piece cost. (c) An estimate, based on the use of vacuum-melted AMS 6265 steel. The actual forging piece cost, based on the use of AMS 6260 (air-melted), was $80.

7 Manufacturing cost of machined ring gears from conventional closed-die and ring-rolled forgings[22]

Ref. 22*. A helicopter steel ring gear was pro-
duced originally by closed-die forging and then
forging was replaced by ring rolling; the cost
analysis presented in Fig. 7 shows that ring roll-
ing has a lower cost largely because stock tooling
that was already available to the forging producer
could be used. In contrast, closed-die forging
included die and set-up costs and an additional
cost resulting from the greater weight of metal
used; the closed-die forging weighed approxi-
mately 4 kg more than the ring-rolled product.
(The costs are based on prices in 1970.)
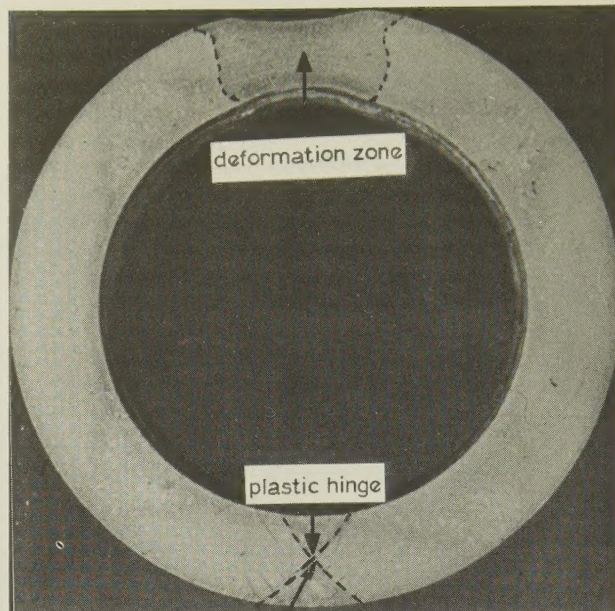
ASPECTS OF MECHANICS

Despite the developing and increasing application
of the ring-rolling process, its mechanics has
received very little attention and the amount of
published work on the subject is very small.

Certain aspects of ring rolling have received
experimental and analytical treatment mainly in
the UK and in the USSR. In the following sections
published work and some results about various
aspects of plain and profile ring rolling are sum-
marized briefly.

Analysis

Analysis developed for roll force and torque in
flat rolling is *not* appropriate for ring rolling
There are significant differences between these
two processes; in the latter the reduction per pass
is relatively small (since the required size is
achieved through a large number of ring rotations)
and the diameters of the rolls are unequal with one
roll undriven. The shape of the plastic region
between the rolls also differs appreciably from
that for flat rolling. Because of the small reduc-
tion per pass the ratio of ring wall thickness to
the length of contact between the workpiece and
roll is generally greater than unity so that the slip-
line field solution for the well known indentation
problem[46] can be used to help predict roll force
and torque when rolling plain rings.[47] The latter
analysis is easily altered to accommodate analys-
ing the rolling of T-shaped sections from an
initially rectangular cross-section, *see* Fig. 3*b*
and Refs. 48–50.

It is assumed that $l_1 \approx l_2 = l$ (Fig. 3*b*), so that
the rolls can be treated as flat indenters of equal
width. The pressure p applied by the indenter
varies between $2k$ and $2k(1 + \pi/2)$ depending on
the ratio of the ring wall thickness H to the con-
tact length l, *see* Fig. 1; plane-strain conditions
are assumed. k is the yield stress of the metal in
plane strain. It is relevant to note that a plastic

---

*Based on producers' experience, the cost of
forgings produced by ring rolling and by closed-
die forging is nearly the same at the low end of
the diameter range (about 18 cm), and changes
gradually in favour of ring rolling as the dia-
meter increases.[22]

8   Indentation of steel ring across its thickness
showing deformation zone and fully formed
plastic hinge

hinge is formed in a ring compressed through its
thickness over a small part of the circumference –
usually at a section opposite the roll gap, *see*
Fig. 8. Small 'back' stresses are imposed in the
roll throat region; *see* the elementary analysis
presented by Johnson *et al.*[51–53]

From the analysis, as discussed in Refs. 47
and 48, expressions for pressure in terms of a
factor γ, for roll force L, and torque T are ob-
tainable. This pressure factor γ is given by

$$\gamma = \gamma_1 + \frac{H}{4D_{\mathrm{m}}} + \frac{\sigma_{\mathrm{h}}}{2k} \qquad \text{for } 1 < H/l \le 8.74$$

and

$$\gamma = \left(1 + \frac{H}{4D_{\mathrm{m}}} + \frac{\sigma_{\mathrm{h}}}{2k}\right)\gamma_2 \qquad \text{for } H/l \le 1$$

γ_1 is obtained from the indentation curve for no
lateral constraint (Fig. 1) and γ_2 provides an
estimate of the influence of friction. D_{oc} and D_{m}
are current outer and mean diameters, σ_{h} is the
compressive hoop stress when rolling T-shaped
rings, and f/N the closure rate for roll revolution
(feedrate). This information can be assembled
conveniently to provide very useful nomograms,
see Fig. 9.

The roll force for T-shaped rings is given by

$$L = 2k\gamma l\,(\overline{W} - b)$$

where $\overline{W}$ is the current mean width of the ring and
b the width of the groove (*see* Fig. 1 of Ref. 48).
The input torque can be expressed as

$$T = 2k\gamma\,(D_{\mathrm{oc}} - H)\,(\overline{W} - b)\,(f/N)$$

9   Nomograph for determining contact length l and pressure factor γ to give roll force and torque

all dimensions are in inches
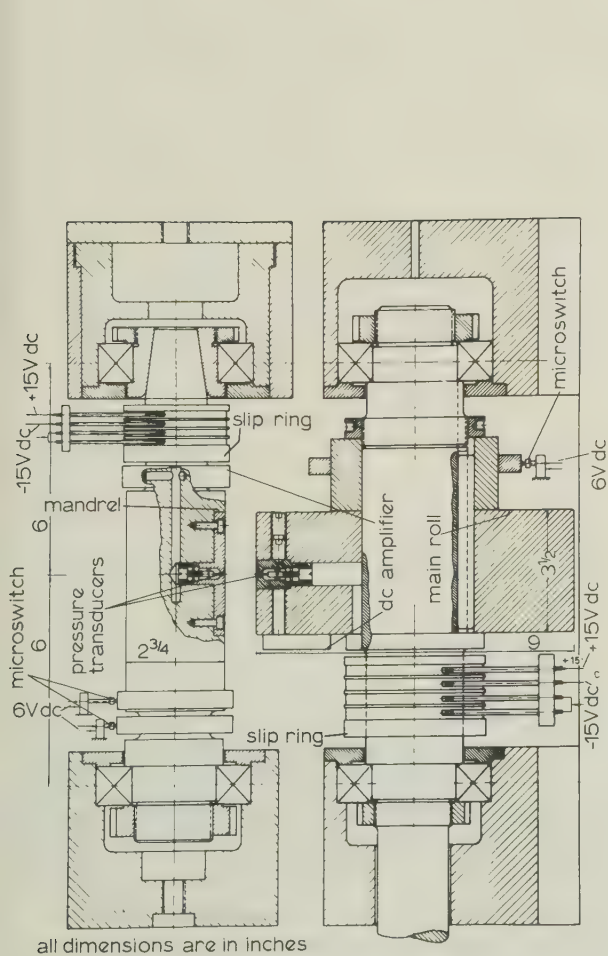
10   Sectional views of rolls
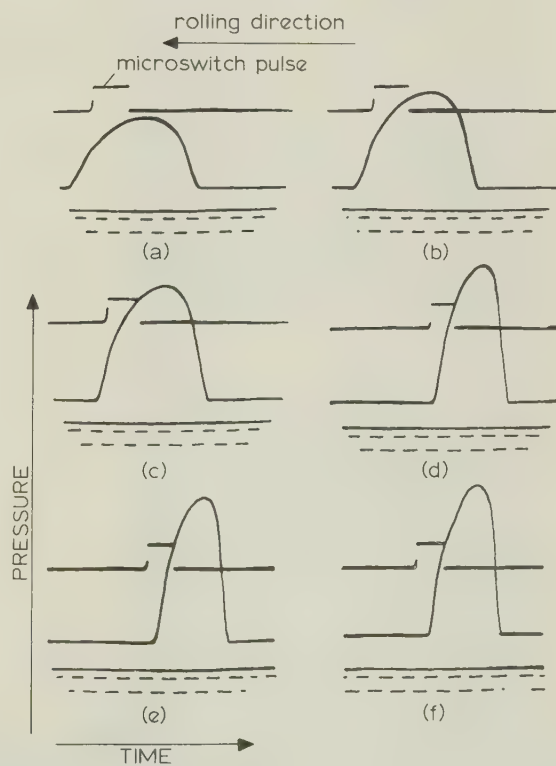
a 5.1%; b 17.3%; c 29.4%; d 44.1%; e 56.3%; f 67.1%

11   Typical uncorrected curves of inside pressure distribution when rolling plain rings at constant feedrate of 4.08 mmrev^{-1} after various total reductions (after Mamalis et al.[48])

a outside pressure, $Z = 0$; *b* outside pressure, $Z = 6.3$ mm; *c* outside pressure, $Z = 12$ mm; *d* inside pressure, $Z = 0$; *e* inside pressure, $Z = 6.3$ mm; *f* inside pressure, $Z = 12$ mm

12   Normal pressure distribution curves when rolling plain rings of annealed Al—0.8Mg—1Si—0.7Mn at constant feedrate of 0.48 mmrev^{-1} with pin located at a distance Z from centreline of axial width of ring after various total reductions: *CL* is line joining roll centres (Mamalis[62])

The driving torque as obtained from the resultant forces and the lever arm is discussed in detail in Ref. 48, but *see* also the work by Tselikov[54] and Teterin and Pukyanov.[55]

The indentation type of analysis has also found application in the Russian work of Smirvov,[56] Ponomarev and Revunov,[57] Polukhin *et al.*,[58] and Solovcov and Al'sic[59] in the case of shaped rings, and by Ostrouskin[60] for plain rings with the main roll in the form of a die.

Some results concerning yield-strength variation of aluminium rings after rolling are given in Ref. 61, but *see* also Ref. 62.

Pressure distribution

In Refs. 48—50 and 63 measurements of normal pressure distribution over the whole area of contact between the roll stock and the rolls during the plain and profile rolling of tellurium lead (simu-

lated hot-rolling conditions) and aluminium-alloy rings (cold-rolling conditions) are reported. Results for the pressure distribution on rings rolled in a conventional 2-high—4-high mill, modified to accommodate ring specimens were reported by Polukhin *et al.*[64,65] and a survey of the main contributions to the literature on the techniques used to find the pressure distribution during various forming processes is also given in Ref. 63.

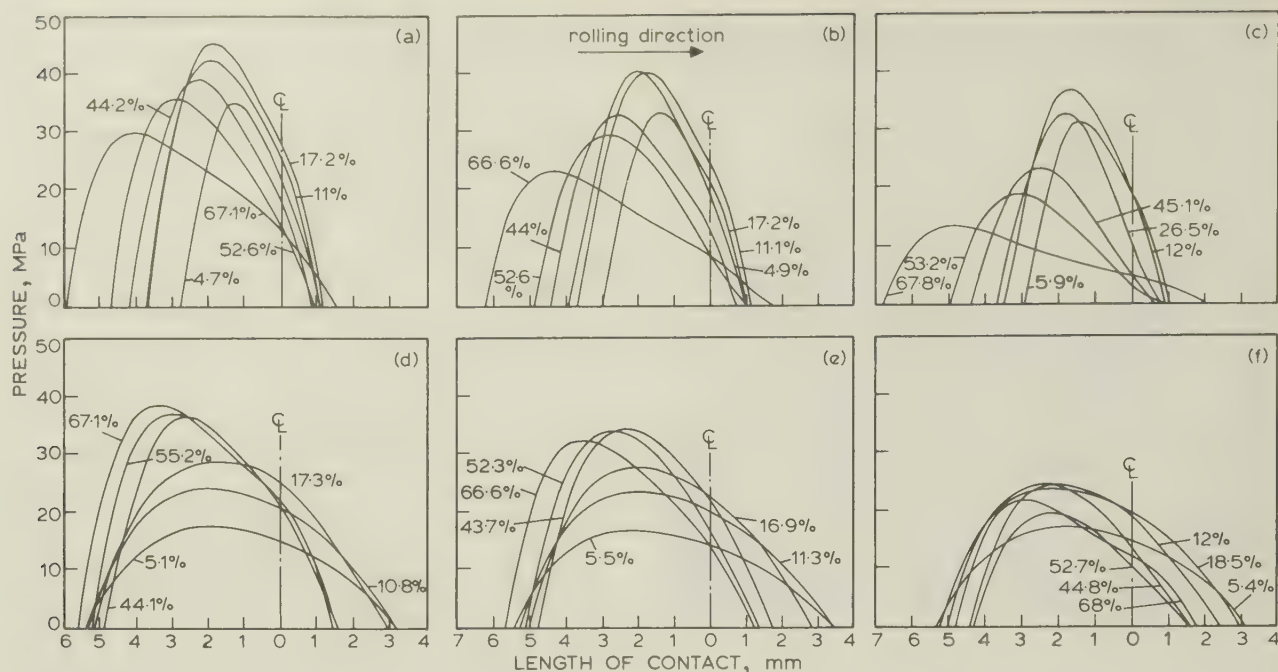To determine normal pressure distribution,[48,63] a pin technique was used, *see* Fig. 10. The pin, with a tip diameter of 1 mm, was fitted radially into the rolls, ending flush with the roll surface where it made contact with the deforming material. Using electroresistance strain gauges, with a continuous-feed camera, pressure—time records were taken.[48,63]

Detailed normal pressure-distribution curves as deduced for successive passes for the faces of

13   Spread profile (fishtail formation) for *a* plain and *b* profiled tellurium lead rings formed from an initially rectangular cross-section, after total reduction given (from right to left) of plain rings: 20%, 29.6%, 39.2%, 46.9%, 57.7%, 64.2%; and profiled rings ($b_0/W_0 = 0.25$): 20%, 29.6%, 39.6%, 47.7%, 57.5%, 63.6%; feedrate 2.54 mmrev^{-1} (Mamalis *et al.*[68])

both rolls when rolling aluminium-alloy plain rings are presented in Figs.11 and 12. The main features of the pressure distribution are[48,63]:

(i) that the pressure (both outside and inside) increases *rapidly* from entry to the roll gap to reach a maximum (peak) and afterwards falls *slowly* towards the exit. The formation of the early peak near to the entry plane contrasts with that of conventional flat rolling, where it appears close to the exit plane[66,67]

(ii) the experimental pressure curve for cold rolling has a more rounded shape in the vicinity of the maximum pressure when com-pared with the rolling of tellurium lead

(iii) for large total reductions a slight 'knee' on the outside pressure curves is observed close to the line joining the roll centres. The total length of contact increases with increas-ing reduction

(iv) in contrast with the outside pressure, the inside pressure curve is flat in the early stages of rolling but is progressively 'com-pressed' towards the position of the line join-ing the roll centres as reduction increases. Similarly, a knee is also observed but more pronounced in the case of fast feedrates (i.e. pressing in of the moving roll) when rolling tellurium lead. For values $H/l_d \approx 1$ (H is the ring thickness and l_d is the length of contact) the pressure curve is irregular with two maxima, one on entering and one just after the line joining the roll centres. The length of contact decreases with increasing reduction

(v) ring geometry is a significant factor in press-ure distribution. It was observed, *see* Refs. 48 and 63, that the outside mean pressure seems to be as given by the slip-line field indentation and that the envelope of all maxima for the inside pressure curves, in relation to total reduction, is a curve similar to that of the flow stress–strain curve of the material itself.

Spread

In commercial ring-rolling operations, the edge shape of the ring is generally controlled by the use of edge rolls or flanges on the main roll. When rolling rings which are unconstrained axially, spreading of the material in this axial direction occurs and an irregular and non-rec-tangular spread profile is developed, i.e. there is a characteristic 'fishtail' appearance, *see* Fig.13.

A detailed account of spread when rolling plain and profiled rings formed from an initially rectangular cross-section is given in Refs.68 and 69. Summarizing the main features of the results reported, the following conclusions may be made:

(i) the spread profile for plain and profiled rings is irregular and non-rectangular, fishtailing taking place in every case. In general, spread
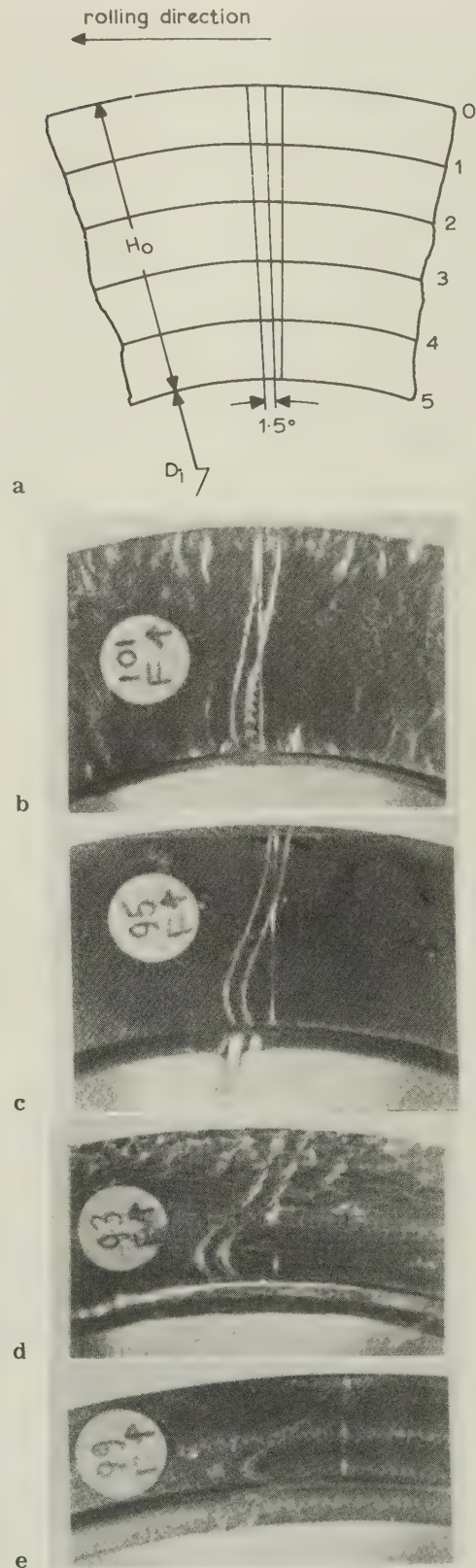
a 0; *b* 20%, *c* 29.6%; *d* 47.7%; *e* 63.9%

14 Deformation patterns (top view) when rolling tellurium lead profiled rings ($b_0/W_0 = 0.25$) at a constant feedrate of 2.54 mmrev^{-1} after total reductions given

increases with increasing total reduction in
ring wall thickness

(ii)   the feedrate has a marked effect on the spread
since, with increasing feedrate, the spread
profile becomes more regular.

An explanation of the fishtail formation[68] can be
had by reference to slip-line field indentation
theory, *see* Fig. 3*b*. It is predicted[68] that tensile
hoop stresses can arise in the central region of
the ring, near A, while compressive stresses
occur close to the working rolls, i.e. near l_1, l_2.
Thus, at the latter extremities the material spreads
axially while in the central regions it expands less
or even contracts. Of course, the final fishtail
shape is the result of a deformation history in
which H/l_1 and H/l_2 decrease continuously.

Typical experimental results for spread in
plain and T-shaped section rolling are shown in
Fig. 13. Some experimental results concerning
spread when rolling flat rings are also reported
in Refs. 70 and 71; *see* also the work by Turon and
Pejčoch[72] on spread when forging and rolling
wheels in mild steel at elevated temperature.

Deformation patterns

Some early but not very accurate attempts to
provide information about the flow of material
during forging and ring rolling were made by
Coron[73] and Weber.[74] Rods of the same material
as the actual specimens were inserted into the
initial ingot and the displacements occurring owing
to deformation were examined after rolling. All
these experiments were carried out on an indus-
trial scale with low-carbon steels at elevated
temperature; *see* also Refs. 75 and 76 and the
work of Lehmann[35] and Shifrin and Solomovich[36]
concerning flow of the material during the manu-
facture of tyres.

An account of the flow of material when
rolling plain and profiled rings is given in Refs.
68 and 69. A fine network of equidistant concen-
tric circles and radii drawn at equal angular
positions was scribed accurately on the top,
bottom, and side faces of an initial blank, while
the flow of the material inside the ring section
was examined by drilling holes axially and radi-
ally and inserting rods of similar material.
Examination of the deformed patterns was made
after rolling the ring to a certain total reduction,
see Figs. 14 and 15.

Concentric circles remain concentric after
the deformation in rolling (apparent in Fig. 14*b*—*e*)
but the distance between them changes owing to
the unequal stretching of the various regions of
the ring; the least stretching occurs at the edge
close to the main roll.[68] Initially, straight radii
are curved in the rolling direction indicating that
in the actual rolling process there are combined
bending and shearing effects which are most
pronounced with fast feedrates. It is also to be
noted that the point at which a change in curva-
ture of the distorted radii occurs, *see* Fig. 14,

15   Distortion in hoop direction of initially
straight tin—lead rod inserted radially at mid
plane of a tellurium lead profiled ring after a
total reduction of 50%, feedrate 0.48 mmrev^{-1}

corresponds to the position of minimum speed in
the central regions of the ring.[68] The deformation
developed inside a ring section is shown in Fig. 15.

Rolling defects

Interestingly, a thin-hooplike cavity—a separation
of the material from the main roll, where, initially,
it was in contact with it—occurs for certain roll-
ing conditions, when rolling profiled T-shaped
rings,[78] *see* Fig. 16. It is noteworthy that this
defect is similar to that of the cavity formation
which occurs in axisymmetric or plane-strain
extrusion during the final unsteady phase of the
process and when the slug thickness has become
greatly reduced, *see* Fig. 9 of Ref. 1. This lifting-
away phenomenon has been noted also by Hill in
his paper on cutting metal strips, *see* Fig. 9 of
Ref. 1; a pipe or gap is created between the
supporting surface and the cut material.

Edge cracking during the ring rolling of
fully heat-treated aluminium alloy and stainless
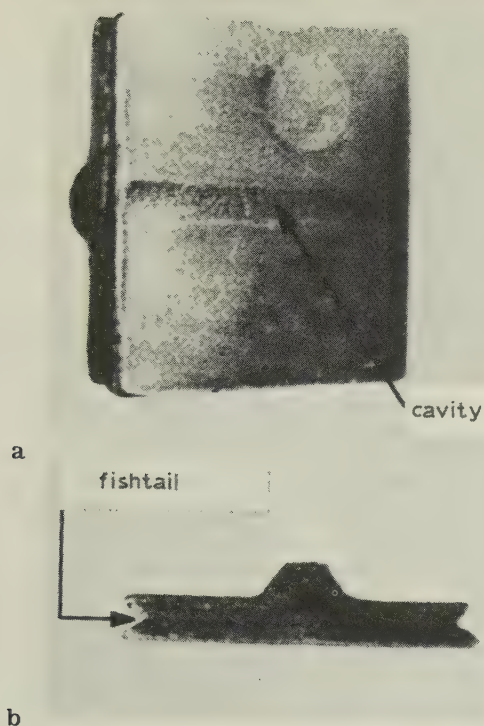
16 Cavity formation when rolling tellurium lead profiled rings ($b_0/W_0 = 0.25$) at a constant feedrate of 0.18 mmrev^{-1} after total reduction of 72%

steel[1] and distortion of the ring into fairly straight-sided forms owing to insufficient rolling load, *see* Fig. 5*d*, have also been observed.[1,70]

CONCLUSION

Flat rolling has been adequately analysed only in the last 30 years (or less) and flat-section rolling is still an art rather than a science. Ring rolling confronts one with an even more complicated geometry and hence a fully satisfactory treatment of most aspects of the plasticity mechanics of ring forming are likely to be long in emerging.

ACKNOWLEDGMENT

REFERENCES

1. W. Johnson and A. G. Mamalis: 'Proc. 17th int. MTDR conf., Birmingham, 1976', (ed. S. A. Tobias), 607; 1977, London, Macmillan.
2. A. G. Mamalis and W. Johnson: *J. Eng. Prod.*, 1978, **2**, 145.
3. F. W. Harboard and J. W. Hall: 'Metallurgy of steel', Vol. 2; 1923, London, Charles Griffin.
4. S. Huffam: British Patent No. 7006, 1884.
5. G. W. Willford: British Patent No. 18456, 1891.
6. H. Muller: British Patent No. 28123, 1896.
7. K. H. Beseler: *Werkstattstechnik,* 1967, **57**, 519.
8. K. H. Beseler: *Konstruktion,* 1967, **19**, 1^1.
9. K. H. Beseler: *VDI-Ber.,* 1968, (123), 141.
10. K. H. Beseler: *Met. Form.,* 1969, **36**, 44.
11. G. Vieregge: *Stahl Eisen,* 1971, **91**, 563.
12. H. J. Marczinski: *ibid.,* 1974, **94**, 1207.
13. H. J. Marczinski: *Metall. Met. Form.,* 1976, **43**, 171.
14. *Iron Age,* 3 Feb. 1966, 64.
15. D. M. Potter: *Aircraft Prod.,* 1960, **22**, 468.
16. *Ind. Heat.,* 1972, **39**, (1), 50.
17. W. Maßberg: *Werkstattstechnik,* 1971, **61**, 346.
18. E. Emilius: *Siemens-Z.,* 1970, **44**, 559.
19. G. Hoffmann: *Fördern Heben,* 1972, **22**, 461.
20. C. H. Meyer: *Stahl Eisen,* 1972, **92**, 120.
21. W. Johnson and J. B. Hawkyard: Paper presented at 5th Int. Cold Forging Cong., Brighton, 1975; *Metall. Met. Form.,* 1976, **43**, 4.
22. 'Metals handbook', 8 ed., Vol. 5, 105; 1970, Metals Park, Ohio, American Society for Metals.
23. M. Abramski: *Wiad. Hutn.,* 1965, **16**, (1), 10.
24. L. Bagni and M. Cinguegrana: 'Freiformschmieden', 119–130; 1966, Düsseldorf, Verlag Stahleisen.
25. S. R. Bartnik, C. W. Mote, and R. L. Bidwell: *SAE J.,* 1962, **70**, (8), 71.
26. J. Motyka: *Pratique Ind. Méc.,* 1966, **49**, 349.
27. *Wiggin Nickel-Rundsch.,* 1965, (7), 3.
28. K. Gale: *Engineer,* 1970, **231**, (5984), 43.
29. J. B. Hawkyard, F. R. Navaratne, and W. Johnson: 'Proc. 15th int. MTDR conf., Birmingham, 1974', (eds. S. A. Tobias and F. Koenigsberger), 507; 1975, London, Macmillan.
30. C. A. Weinert: *Automot. Ind.,* 1970, **142**, (11), 33.
31. P. F. Egan: 'Proc. 14th int. MTDR conf., Manchester, 1973', (eds. S. A. Tobias and F. Koenigsberger), 759; 1974, London, Macmillan.
32. J. Mortimer: *Engineer,* 30 Jan. 1975, **240**, 20.
33. H. Finke: *Kugellager-Z.,* 1963, **38**, (138), 9.
34. R. E. Green: *Machinery (New York),* 1963, **69**, (12), 92.
35. O. H. Lehmann: 'Die Herstellung von Radreifen, Radscheiben und Vollrädern'; 1952, Düsseldorf, Verlag Stahleisen.
36. M. Yu. Shifrin and M. Ya. Solomovich: 'Proizvodstvo tsel'nokatanykh kolets i bandazhei'; 1954, Moscow, Metallurgizdat.
37. M. Yu. Shifrin: *Metallurg,* 1961, (5), 28.
38. M. Yu. Shifrin: *Izv. VUZ Chernaya Metall.,* 1969, **12**, (1), 101.
39. T. S. Makaeva and V. A. Parshin: *Stal in English,* Feb. 1965, 123.
40. B. Volf and P. Milan: *Hutnik (Prague),* 1970, **20**, (12), 465.

41. J. T. Winship: *Am. Machinist,* 1975, **119**, (18), 62.
42. J. T. Winship: *ibid.,* 1976, **120**, (1), 110.
43. R. C. Brooks: US Patent Appl. No. 625461, 1975.
44. T. Nakagawa and Y. Suyama: Paper presented at Spring Conf. on 'Powder metallurgy', Tokyo, 1975.
45. H. S. Nayar: 'Modern developments in powder metallurgy', Vol. 6, 'Applications and processes', (eds. H. H. Hausner and W. E. Smith), 155; 1974, Princeton, NJ, Metal Powder Industries Federation.
46. R. Hill: 'The mathematical theory of plasticity'; 1950, Oxford, Clarendon Press.
47. J. B. Hawkyard, W. Johnson, J. Kirkland, and E. Appleton: *Int. J. Mech. Sci.,* 1973, **15**, 873.
48. A. G. Mamalis, W. Johnson, and J. B. Hawkyard: *J. Mech. Eng. Sci.,* 1976, **18**, 11.
49. A. G. Mamalis, W. Johnson, and J. B. Hawkyard: *Metall. Met. Form.,* 1976, **43**, 132.
50. A. G. Mamalis, W. Johnson, and J. B. Hawkyard: *Arch. Eisenhüttenwes.,* 1976, **47**, 613.
51. W. Johnson and G. Needham: *Int. J. Mech. Sci.,* 1968, **10**, 95.
52. W. Johnson and G. Needham: *ibid.,* 487.
53. W. Johnson, I. MacLeod, and G. Needham: *ibid.,* 455.
54. A. I. Tselikov: 'Stress and strain in metal rolling'; 1967, Moscow, MIR Publishers.
55. P. K. Teterin and V. P. Pukyanov: *Kuznechno-Shtampov.,* 1966, (6), 9.
56. V. V. Smirnov: 'Untersuchung der Kräfte beim Warmwalzen von Wälzlagerringen', Sammelband 'Walzwerke und Walztechnologie', No. 62, 74–108; 1955, Moscow, Mashgiz.
57. N. I. Ponomarev and V. A. Revunov: 'Walzen von ringförmigen Ausgangsteilen', Sammelband 'Ausrüstung für das Walzen von Werkstucken komplizierter Form', Chap. IV, 176; 1963, Moscow, Cintiam.
58. P. I. Polukhin, P. K. Teterin, M. M. Shalyapin, and V. K. Vorontsov: *Izv. VUZ Chernaya Metall.,* 1971, (7), 64.
59. S. S. Solovcov and M. Ja. Al'šic: *Kuznechno-Shtampov.,* 1970, (2), 1.
60. G. P. Ostrouskin: *ibid.,* 1973, (4), 5.
61. R. M. Caddell, G. Needham, and W. Johnson: *Int. J. Mech. Sci.,* 1968, **10**, 749.
62. A. G. Mamalis: PhD thesis, University of Manchester, 1975.
63. A. G. Mamalis, W. Johnson, and J. B. Hawkyard: *J. Mech. Eng. Sci.,* 1976, **18**, 184.
64. P. I. Polukhin, P. K. Teterin, M. M. Shalyapin, and V. K. Vorontsov: *Izv. VUZ Chernaya Metall.,* 1970, (11), 77.
65. P. J. Polukhin, P. K. Teterin, M. M. Shalyapin, and V. K. Vorontsov: *Steel USSR,* July 1972, 546.
66. E. Siebel and W. Lueg: *Mitt. K.-Wilh. Inst. Eisenforsch.,* 1933, **15**, 1.
67. C. L. Smith, F. H. Scott, and W. Sylwestrowicz: *J. Iron Steel Inst.,* 1952, **170**, 347.
68. A. G. Mamalis, J. B. Hawkyard, and W. Johnson: *Int. J. Mech. Sci.,* 1976, **18**, 11.
69. A. G. Mamalis, W. Johnson, and J. B. Hawkyard: *Arch. Eisenhüttenwes.,* 1976, **47**, 619
70. J. B. Hawkyard, E. Appleton, and W. Johnson: 'Proc. 13th int. MTDR conf., Birmingham, 1972', (eds. S. A. Tobias and F. Koenigsberger), Paper 85; 1973, London, Macmillan.
71. P. I. Polukhin, P. K. Teterin, M. M. Shalyapin, and V. K. Vorontsov: *Izv. VUZ Chernaya Metall.,* 1972, (9), 69.
72. S. Turon and O. Pejčoch: *Hutn. Listy,* 1963, **10**, 638.
73. P. Coron: *Rev. Métall.,* 1955, **32**, 917.
74. K. H. Weber: *Stahl Eisen,* 1959, **79**, 1912.
75. T. R. Kay, J. B. Lee, and K. W. Andrews: 'Principles of ring rolling', Rotherham Works Trial No. 3023, British Steel Corporation, Report No. PGM/6252/2/72/A, 1972.
76. O. Ulrych: 'Technologie des Walzvorganges und Hinweise für die Werkzeuggestaltung', Rheinstahl Wagner Report, Dortmund, 1968.
77. A. G. Mamalis, J. B. Hawkyard, and W. Johnson: *Int. J. Mech. Sci.,* 1975, **17**, 69.

Physical and chemical nature of cemented carbides

by H. E. Exner

Cemented carbides are, from a technical point of view, one of the most successful composite materials. The physical and chemical aspects of the components (transition-metal carbides and iron-group metals) and of their interaction in hard-metals are reviewed with emphasis on the materials science point of view focusing on those compositions which have gained technical interest. Crystal structures and phase relationships are discussed in detail. The interaction of components (wetting, residual stresses) and some microstructural aspects (size, contiguity, and shape) are treated also. These fundamentals are the basis of understanding the production processes and the properties of cemented carbides.

Cemented carbides (or hardmetals, sometimes also called less appropriately sintered carbides) are a group of sintered materials, the outstanding properties of which are high hardness and wear resistance. The success of cemented carbides in technical application is closely related to their method of manufacture. Brittle refractory carbides of the transition metals (such as WC, TiC, TaC, Cr_3C_2 or Mo_2C) are combined with a tough binder metal (most often cobalt, in some cases nickel or other metals from the iron group). Typical microstructures of commercial alloys are shown in Fig. 1. In these combinations the positive properties of the components are superimposed; the main component (carbide phase) provides hardness and wear resistance while the ductile binder contributes the toughness necessary for most applications. 'Tailor-made' composite materials in which the advantageous properties of the components are combined have been a concept to which extensive technical and scientific effort has been devoted during the last decade. However, most attempts in this direction have not lived up to expectations owing to the fact that the negative properties of the components are usually retained as well. Optimized properties as in the case of cemented carbides are seldom achieved.

H. E. Exner is in the Max-Planck-Institut für Metallforschung, Institut für Werkstoffwissenschaften, Stuttgart, West Germany.

The history of cemented carbides began in Germany during the first World War with successful attempts to produce drawing dies from tungsten carbide. The decisive breakthrough was achieved by Schröter in the early 1920s probably following a proposal by Skaupy. Powders of tungsten carbide and cobalt were mixed and dense parts prepared by compacting the mixture and by heating the compacts above the melting point of the binder phase. Today, it is practically impossible to say whether this discovery was derived from a theoretical concept or was essentially a result of good luck. The first patent in the field of sintered cemented carbides was issued in 1923 followed by numerous others.[1,2] From the beginning, cemented carbide technology was backed up by considerable research activity. Reviews on the achievements of basic research in the field of hardmetals were published recently.[3–7] The rapid development of WC–Co alloys was expanded to other combinations. With multiple-carbide alloys based on mixtures of WC–TiC with additions of (Ta, Nb)C, high-speed machining of steel became possible. A large part of these later developments took place in the USA, in Austria, in Sweden, and, more recently, in Japan, although most of the key inventions had been made in Germany. During the second World War, because of a shortage of tungsten, the discovery of and large-scale production of tungsten carbide-free hardmetals with titanium carbide as the main component was also started in Germany. From this group, titanium carbide–nickel alloys with additions of molybdenum carbide are still used for the shaping of materials which wear tools rapidly.

As shown in Table 1, the historical development of cemented carbides follows three lines:

(i) improvement of tungsten carbide-based alloys achieved by addition of further carbides and alloying the binder phase, by the development of submicrometre tungsten carbide alloys, by hot isostatic recompaction after liquid-phase sintering to reduce the amount of flaws and porosity, and by other refined production techniques

(ii) tungsten-free alloys finding increased technical interest owing to their advantages for special applications and to concern over supplies of raw material

(iii) important discoveries closely related to cemented carbide technology either resulting in competitive products (e.g. ceramic cutting tools) or expanding and/or improving the classic cemented carbides (e.g. carbonitride and boride hardmetals or surface-treated WC—Co alloys).

From a technical point of view, WC-base hardmetals are by far the most important group. The literature on WC—Co, WC—TiC—Co, and TiC—Ni alloys is very large and impossible to review comprehensively. However, preference will be given in this review to these alloys. Other compositions will be considered occasionally and achievements of the third line of developments mentioned above (Table 1, 'Related developments') will be mentioned only briefly. Carbide-free hardmetals are outside the scope of cemented carbides by definition. Other cutting or wear-resistant materials usually not regarded as falling

within this material group are cast carbide-containing alloys (e.g. the classic Stellites or the recently developed W—Ti—Ta—C—Co alloys used for heavy machining) and high-binder alloys (e.g. the so-called Ferro-TiC alloys on the basis of TiC with 50—70 wt-% heat-treatable binder steel or sintered high-speed steels with increased carbide content). Coating and surface-hardening treatments will not be considered since these processes (e.g. chemical vapour deposition) are usually carried out with finished carbide tools outside the traditional production line.

A further restriction is necessary to keep this review within reasonable limits: technical details will be considered only briefly. All industrial aspects of cemented carbide production have been reviewed extensively in the 'World directory and handbook of hardmetals' by K. J. A. Brookes.[2] There, the industrial manufacture of all the technical cemented carbide grades, their properties

Table 1　Development of hardmetals, compiled from Refs. 1—3

Year(s)	WC-base sintered alloys	Year(s)	TiC- (and TaC)-base sintered alloys	Year(s)	Related developments
1922—25	WC+Co (Widia*)	1929—31	TiC—Mo$_2$C+Ni, Cr, Mo (Titanit*)	1909	Stellites
1927	Graphite-free WC+Co			1914	Molten sintered and hot-pressed WC
1928—29	WC with stellite binder	1930—31	TaC+Ni, Co (Ramet*)	1917	Hot-pressed W—Cr—Ti—Fe—C alloys (Tizit*)
1931	WC—TiC+Co (Widia X*)	1931	TiC—TaC+Co		
1931	WC—TaC+Co (Carboloy*)	1931	TiC+Cr, Mo, W, Ni, Co (Böhlerit*)	1922	Infiltrated WC
1932	WC—TiC—(Ta, Nb)+Co (Firthite*)	1938	TiC—VC+Ni, Fe	1930—31	Boride, and boride—nitride and boride—carbide hardmetals
1938	WC—Cr$_3$C$_2$+Co	1944	TiC—NbC+Ni, Co		
1951	Acid-resistant WC—Ni	1948—50	TiC—(Mo$_2$C, TaC)+Ni, Co(Cr)	1950—51	Infiltrated TiC-base alloys
1956	WC—TiC—Ta(Nb)C—Cr$_3$C$_2$+Co	1949	TiC—VC—NbC—Mo$_2$C+Ni	1952—61	TiC+heat-treatable steel (Ferro-TiC*)
1959	WC—TiC—HfC+Co	1965—70	(TiC—Mo$_2$C)-mixtures +Ni, Mo	1953—55	Commercial boride hardmetals
1965	Hot isostatic compaction	1968—70	Solid-solution and precipitation-hardened alloys (Ti, Mo)C+Ni, Mo	1955—60	Ceramic cutting materials (Al$_2$O$_3$ and Cr$_2$O$_3$ with TiC, TiB$_2$, WC, or Mo$_2$C)
1967—70	Submicrometre WC+Co			1955—73	Surface coatings on WC+Co (TiC, TiN, Al$_2$O$_3$, diamond)
1967—70	WC—Fe, Ni, Co			1961—70	Ti(C, N)—Ni, TiN—Ni
1968	WC—TiC—TaC—NbC+Co			1970	Thermochemical surface treatment
				1970 to present	Cast hardmetals

*These names are trade names of products first developed by a specific company and often still used in practice.
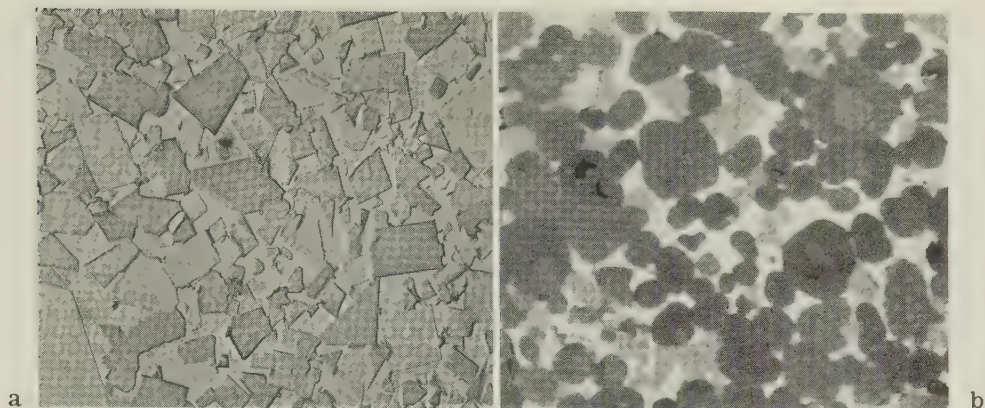
a WC—10 wt-%Co alloy: Formvar replica, electrolytic etch, ×3000; *b* TiC—WC—TaC—Co alloy: electron emission photograph (Balzers Methioscope) ×3200

1 Microstructure of technical grades of cemented carbides

and routine testing, the methods of shaping, finishing, and joining, as well as applications in the machine shop, in rock drilling, and in other fields are covered. The book also gives indexes to hardmetal specifications, to companies and trade names, and to current commercial grades. The present review will be focused on the materials science point of view and is intended to provide the background for understanding the physical and chemical nature of the components and their combinations. It will be followed by reviews on the metallurgical aspects of the preparation (mixing, liquid-phase sintering, etc.) and the physical and mechanical properties of cemented carbides.

STRUCTURES AND PROPERTIES OF TRANSITION-METAL CARBIDES

From the large group of metallic refractory compounds reviewed extensively in the classic book 'Hartstoffe' by R. Kieffer and F. Benesovsky,[8] (carbides, borides, nitrides, and silicides of transition metals) the carbides are used as the hard component of hardmetals almost exclusively. In the past, only some boride-containing alloys have progressed beyond the laboratory stage,[1] and recently, nitride and carbonitride alloys have been claimed to show promise for industrial application.[9-12] Owing to their outstanding combination of properties, however, carbides will not be replaceable to any great extent in the near future.

The properties of refractory carbides have been summarized in a series of standard books.[8,13-21] Some of the properties are collected in Table 2. The most essential features relating to cemented carbides are discussed below.

Tungsten carbide and other VIa-metal carbides

It is well established that tungsten forms two hexagonal carbides, the monocarbide WC and the

Table 2 Some properties of refractory carbides used in cemented carbides

| Carbide	Crystal structure	Lattice parameter*, nm	Melting temperature*, °C	Nominal carbon content, wt-%	Microhardness*, HV (50 g)	Theoretical density, g cm^{-3}	Modulus of elasticity, GN m^{-2}	Coefficient of thermal expansion, 10^{-6} K^{-1}
TiC	fcc	0.433	3100	20.05	3000	4.94	451	7.7
ZrC	fcc	0.470	3400	11.64	2700	6.56	348	6.7
HfC	fcc	0.465	3900	6.30	2600	12.76	352	6.6
VC	fcc	0.417	2700	19.08	2900	5.71	422	7.2
NbC	fcc	0.447	3600	11.45	2000	7.80	338	6.7
TaC	fcc	0.445	3800	6.23	1800	14.50	285	6.3
Cr$_3$C$_2$	orthorhombic	a 0.283 b 0.554 c 1.147	1800†	13.33	1400	6.66	373	10.3
Mo$_2$C	hexagonal	a 0.300 c 0.473	2500	5.89	1500	9.18	533	7.8
WC	hexagonal	a 0.291 c 0.284	2800†	6.13	(0001) 2200 (10Ī0) 1300	15.70	696	5.2 7.3

*Data from Refs. 1 and 13 (approximate values).   †Not congruently melting, dissociation temperature.

subcarbide W_2C. The phase relationships in the tungsten—carbon system have been studied by numerous authors (for early work *see* Refs. 8, 14, 21) but only more recent work has shown that the phase diagram is more complicated than previously assumed owing to the modification changes of W_2C and an additional phase, the cubic substoichiometric WC_{1-z} (Refs. 22-24). Figure 2 shows the tungsten-rich part of the equilibrium diagram for the W—C system. The temperature of the eutectoid reaction $W_2C \rightarrow WC + W$ has been fixed at 1575 ± 5 K by means of activity measurements.[22] However, W_2C is usually retained at room temperature even at slow cooling rates and can easily be produced by melting or by carburization of tungsten. The low-temperature modification is disordered hexagonal, the ordering states of the high-temperature phases are not yet well established. The cubic subcarbide WC_{1-z} is found at room temperature only in extremely rapidly cooled samples, e.g. in plasma-sprayed layers.[25]

As far as cemented carbides are concerned, the high-temerature phases have no importance except during the production of WC where W_2C is obtained as an intermediate product. Figure 3 shows the reaction zones during the formation of WC from a mixture of coarse tungsten powder and carbon black, and Fig. 4 shows the kinetics of this process.[26,27] It is interesting to note that W_2C is obtained far below the minimum temperature of the stable phase which throws some doubts on the eutectoid reaction shown in Fig. 2.

Tungsten monocarbide WC takes the most prominent place of all hard phases in cemented carbides. More than 98% of all hardmetal grades contain WC, and more than half of these are pure WC—Co alloys.[28] Owing to the fact that WC melts incongruently, (i.e. decomposes before melting, *see* Fig. 2) it can not be produced by melting. The preferred way of production (by which an annual tonnage of about 10 000 t is made) is the reaction of pure tungsten powder (>99. 9 wt-%) with carbon black of low ash content. The tungsten powder used in cemented carbide technology is usually produced by reduction of tungsten trioxide WO_3, tungsten hydratic acid H_2WO_4, blue tungsten oxide W_4O_{11}, or ammonium paratungstenate $5 NH_3 . 12 WO_3 . 5 H_2O$. Coarse and polycrystalline WC powders (particle size >2 μm) are obtained from coarse W powders (>6 μm) at relatively high carburization temperatures (usually 1600°C) while fine and essentially monocrystalline WC (particle size <1 μm) is produced from submicrometre tungsten (particle size <0. 1 μm) at 1350°— 1400°C. In small quantities, superfine WC is obtained by reactions in gaseous phases, e.g. by the Axel—Johnson process[29] or the Ciba process.[30] Finally, the menstruum technique[31] based on old patents must be mentioned. As shown by Kieffer and co-workers,[31-34] very pure (oxygen reduced by a factor 10) and well crystallized carbides can be obtained by this process, which consists of dissolving the transition melts in a graphite-covered melt of iron, nickel, or cobalt (the so-called 'auxilary bath') and extracting the carbide crystals from the cooled and crushed material by
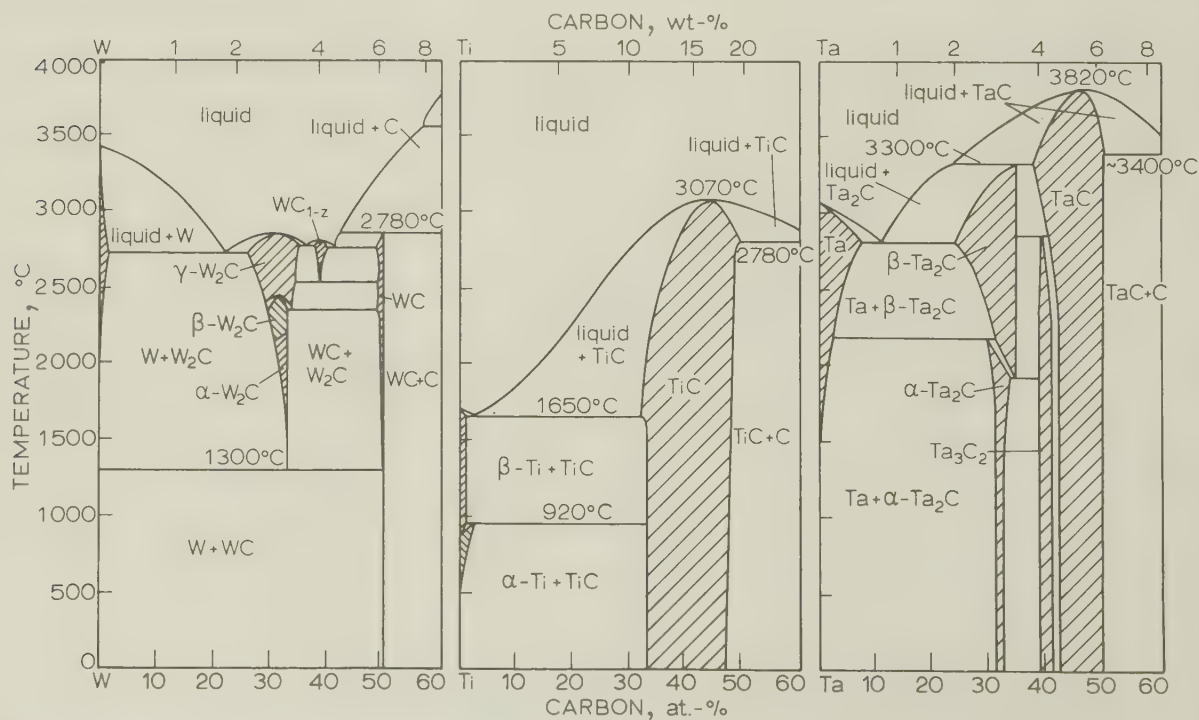

2 Phase diagrams of *a* **W—C,** *b* **Ti—C, and** *c* **Ta—C systems**
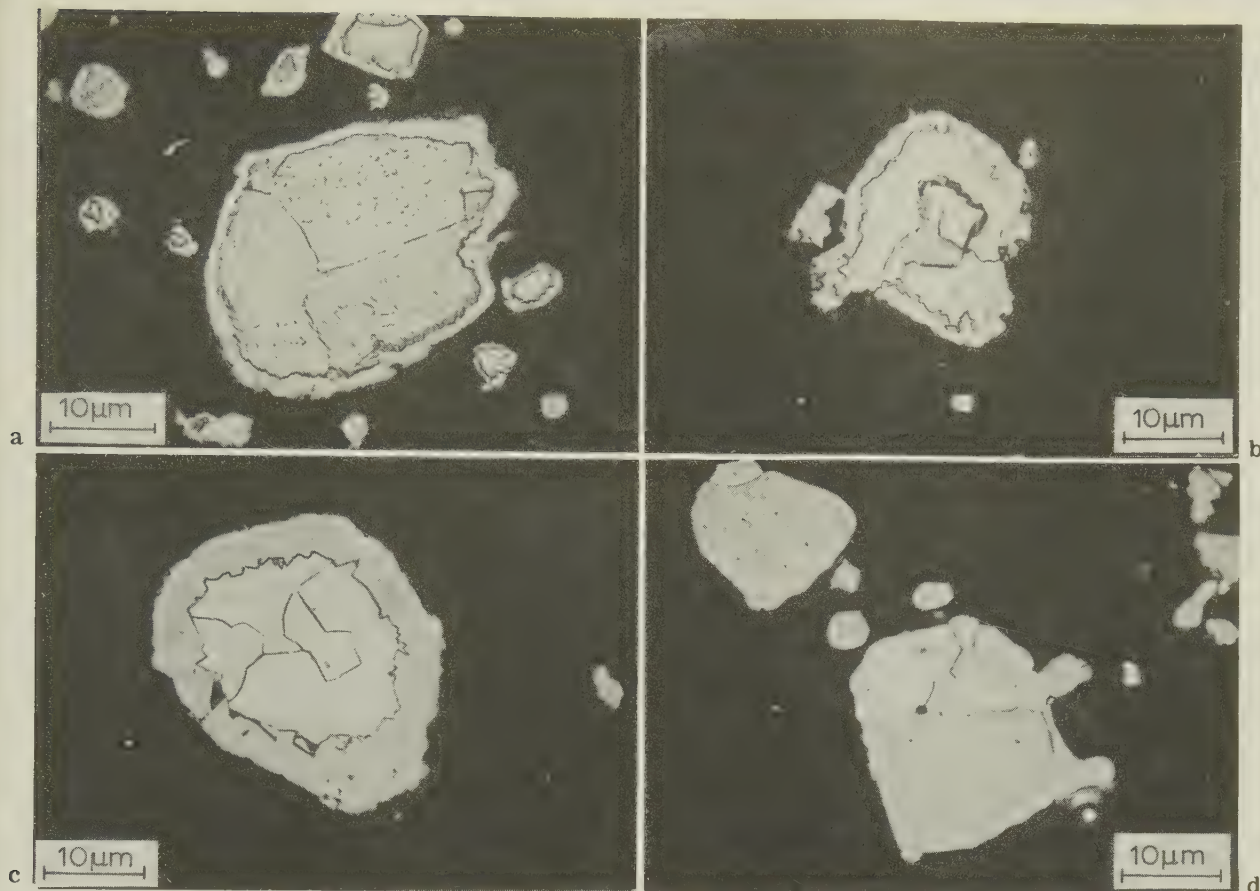
a carburized at 1200°C, tungsten surrounded by WC; *b* carburized at 1400°C, tungsten (centre), W_2C, (outer layer); *c* carburized at 1500°C, W_2C (centre), WC (outer layer); *d* carburized at 1900°C, WC particles with large grains
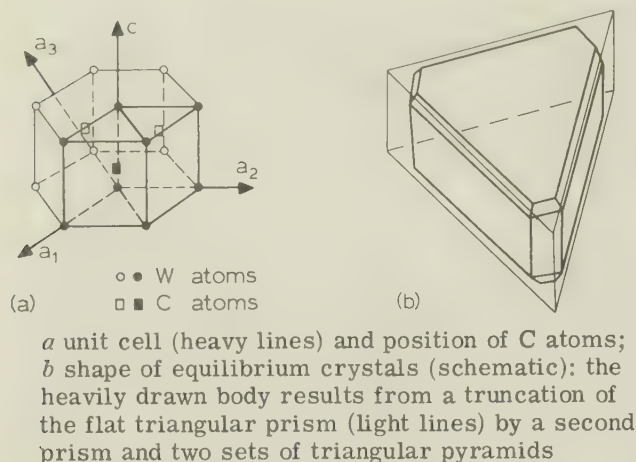
3 Reaction products during carburization of tungsten (reaction time 20 min), after Hara and Miyake[26,27]
$$\times 3000$$

an acid treatment. The preparation conditions determine not only the particle size of the carbide powders but also their wetting and growth behaviour during sintering and the properties of the carbide grains in the cemented carbide alloys. This influence of the chemical history must be kept in mind as an important parameter in hard-metal production.
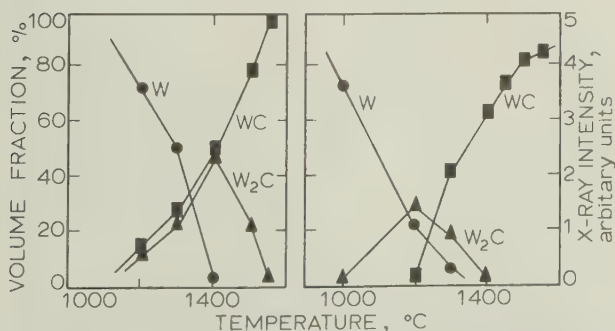
4 Kinetics of formation of W_2C and WC during reaction of coarse tungsten powder with carbon black, after Hara and Miyake[26,27]

Another important feature of the W—C phase diagram (Fig. 2) is the very small range of homogeneity of WC. The carbon content corresponds to the theoretical value of the stoichiometric composition (50 at.-% or 6.13 wt-%C). This means that there are neither carbon nor tungsten vacancies or interstitials other than those created by thermal activation. The crystal structure is simple hexagonal with two atoms per unit cell (Fig. 5a); the lattice constants are $a = 0.2906$ nm and $c = 0.2837$ nm with $c/a = 0.976$.[35,36] The prism crystal planes of $(10\bar{1}0)$-type are highly polar because of the different spacings of the tungsten and carbon planes $[10\bar{1}0]$ direction, and there are two sets of three equivalent $(10\bar{1}0)$ planes rather than six equivalent $(10\bar{1}0)$ planes.[37] This is the reason why WC crystals grown from liquid-metal solutions assume the typical shape shown in Fig. 5b,[37-42] which corresponds to the ditrigonal-bipyramidal class of the crystal system.[38] This is also the equilibrium shape of the WC grains in cemented carbides[42-46] and the WC-grain intersects in polished WC—Co or WC—TiC—Co samples show the typical shape of plane sections of such crystals (*see* Fig. 1 and the section 'Microstructural aspects' below).

a unit cell (heavy lines) and position of C atoms; *b* shape of equilibrium crystals (schematic): the heavily drawn body results from a truncation of the flat triangular prism (light lines) by a second prism and two sets of triangular pyramids
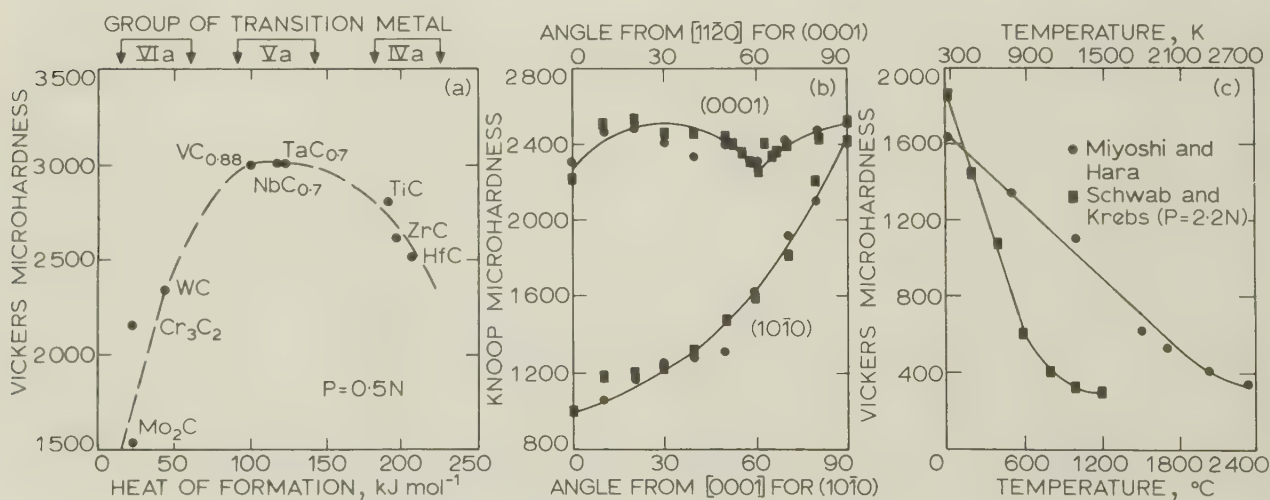
5 Crystal structure of WC

Considering the properties of WC, it is not obvious why this carbide retains first place ahead of all other carbides in cemented carbide technology. Its thermodynamic stability is relatively low (standard free energy of formation 40 ± 2 kJ mol^{-1} at 25°C (Ref. 14) or $-42.3 \pm 0.005T$ kJ mol^{-1} in the temperature range 1150 K $< T <$ 1575 K (Ref. 22)). As shown in Fig. 6*a*, only the other two carbides of the VIa-group metals (Cr_3C_2 and Mo_2C) are less stable, while the cubic carbides of the IVa- and Va-group metals have much higher heats of formation.[47] Also shown in Fig. 6*a* is a comparison of the microhardness of these carbides: the WC values are well below the maximum hardness values of the cubic carbides. In accordance with the non-centrosymmetric crystal structure, the microhardness of WC is highly

anisotropic.[40,42,52] As shown in Fig. 6*b*, the Knoop hardness on the basal plane (0001) varies from 2200 in the $[11\bar{2}0]$ direction to 2500 at an angle of 30° to this direction with a threefold symmetry, and on the prism planes $(10\bar{1}0)$ from only 1000 in the [0001] direction to 2400 at 90° to this direction with a twofold symmetry.[48] It is not surprising that microhardness values measured at arbitrary orientations show a large scatter, and that room-temperature microhardness values given in the literature (e.g. Refs. 49–51, for earlier work *see* Refs. 8, 48) have a wide range. Microhardness decreases linearly with increasing temperature in the technically interesting temperature range (Fig. 6*c*) showing marked softening of WC at temperatures easily reached during metal cutting. As shown in Fig. 6*c*, there are considerable deviations in experimental results obtained by different authors.[49-51] Attempts have been made to explain the high hardness of carbides and its temperature dependence (*see* e.g. Ref. 51) but none of these is established well enough to provide more than a useful working hypothesis.

Until the mid 1960s WC was assumed to be perfectly brittle. This assumption led to a still persisting controversy on the degree of skeleton formation in cemented carbides (*see* e.g. Ref. 44). There is a lot of evidence, however, that WC shows appreciable plastic deformation. The formation of slip bands has been observed in the vicinity of hardness indentations in WC single crystals.[38-42,47,52-55] Glide bands and dislocation-network formation indicate that the WC grains in WC–Co alloys are plastically deformed during compression testing and even during transverse rupture testing as shown by numerous investigators.[37,56-73] The minimum stress re-

a maximum Vickers microhardness of IVa-, Va-, and VIa-metal carbides as function of heat of formation, after Ramqvist[47]; *b* Knoop microhardness as function of lattice orientation, after French and Thomas[48] (square symbols indicate values obtained for symmetric angles in range between 90° and 180°; *c* temperature dependence of microhardness of WC, after Miyoshi and Hara[49,50] and Schwab and Krebs[51]

6 Microhardness of transition-metal carbides
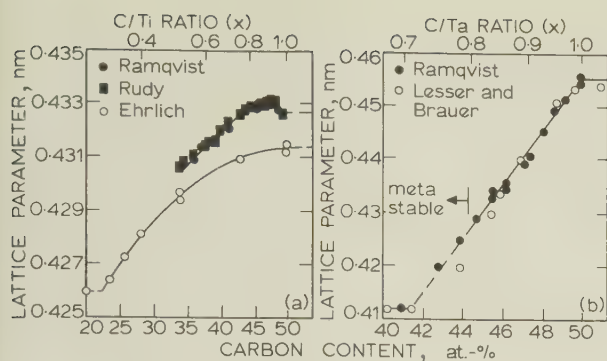
a titanium carbide TiC$_x$, after Ramqvist[91] (samples produced by arc melting), Rudy[24] (samples produced by quenching from slightly above solidus and annealing at 1350°C), and Ehrlich[92] (samples produced by sintering); *b* tantalum carbide TaC$_x$, after Ramqvist[93] (samples produced by gas carburization or hot pressing) and Lesser and Brauer[94] (samples produced by vacuum carburization)

7 Lattice parameter of transition-metal carbides as function of carbon content

quired to propagate slip in WC crystals has been estimated at 1500 MN m^{-2} (Refs. 41, 74); however, more work is needed to define the yield strength of WC. The prism planes (10$\bar{1}$0) have been identified as slip planes and [0001] and $\frac{1}{3}$[11$\bar{2}$0] as Burgers vectors.[37,40,48,56,57,60] An additional slip system (1010) with the Burgers vector [1123] has been reported,[37,58] which consists of unit dislocations of Burgers vector $\frac{1}{6}$[20$\bar{2}$3] and $\frac{1}{6}$[0223], respectively. These plastic properties of the WC crystals explain at least partially the macroscopic plastic deformation of WC—Co alloys while the formation of dislocation networks was assumed to result in work hardening[59] and a smaller hardness loss with temperature than that exhibited by the cubic refractory-metal carbides *see* below.

Other essential features of WC are the extremely high modulus of elasticity, well above 700 GN m^{-2}, (Refs. 8, 75, 76) a value exceeded only by diamond,[28] and its high thermal conductivity of 1.2 J cm^{-1} s^{-1} K^{-1} (Ref. 77), both advantageous properties in cutting applications. The strength of pure WC is not well established,[8] but it is important to note that the yield strength as well as the fracture strength of individual carbide particles seems to decrease with increasing particle size.[60,78]

A general theoretical explanation of the properties of WC from an electronic point of view is as yet not available because of the complex nature of bonding forces.[37,47,79] More work is needed here, especially for future developments where other hard materials may be substituted for WC in cemented carbides.
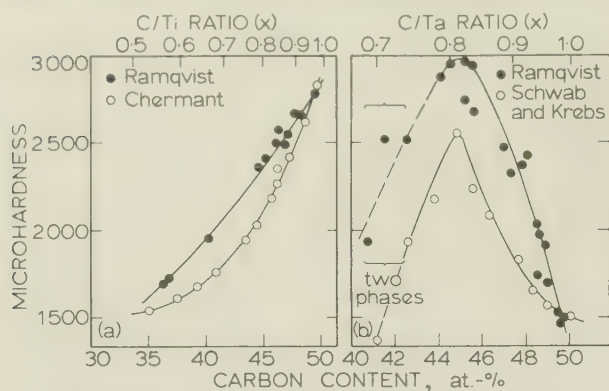
Two more carbides of the VIa metals have some importance in cemented carbide technology, the hexagonal molybdenum carbide Mo$_2$C, and the orthorhombic chromium carbide Cr$_3$C$_2$. Both have a narrow range of homogeneity. Mo$_2$C has a stoichiometric carbon content of 5.89 wt-% and melts congruently at about 2500°C according to more recent literature.[19] It is usually produced by carburization of molybdenum oxide powder (MoO$_3$ or MoO$_2$) with carbon black under hydrogen at 1300°—1500°C. It is much cheaper than WC but less hard and more brittle. Cr$_3$C$_2$ disintegrates before melting at about 1900°C. It has a stoichiometric carbon content of 13.3 wt-% and a high solubility in nickel and cobalt (about 11 wt-% at 1250°C). The main advantages of Cr$_3$C$_2$ are its unique oxidation and corrosion resistance, its comparatively very low price, and its easy availability. Again it is more brittle and less hard than WC. The use of both carbides in conventional hardmetals is limited to small additions mainly for grain refinement owing to their embrittling action. Mo$_2$C is a main constituent of TiC grades with Ni binder for fine machining and extreme wear applications; Cr$_3$C$_2$ is used with Ni binder for corrosion-resistant hardmetals.

Titanium carbide, tantalum carbide, and other cubic carbides

Metals of the IVa group of the periodic table form only one carbide each (TiC, ZrC, and HfC). The Va metals also form monocarbides (VC, NbC, and TaC) and, additionally, carbides of lower carbon content which, however, have found no application in cemented carbide technology. The monocarbides are all face-centred cubic, they melt congruently, and are harder than WC (*see* Fig. 6a and Table 2). The properties and the metallurgical behaviour of the carbides in each group are very similar. In the following, TiC and TaC are chosen to represent the IVa- and the Va-metal carbides, respectively, since these are used frequently in cemented carbides while the other carbides are of limited interest.

The metal-rich parts of the phase diagrams of the Ti—C and Ta—C systems[14,19,24] are shown in Fig. 2. The monocarbides have a wide range of homogeneity and their maximum carbon content is somewhat less than (IVa-metal carbides) or at (Va-metal carbides) the stoichiometric composition. Carbon deficiency, therefore, does not produce an extra phase in hardmetals containing higher amounts of cubic carbides.

The simple crystallographic structure of the monocarbides makes them especially suitable for theoretical investigations on the nature of binding forces, and a considerable amount of work has been devoted to this problem (*see* e.g. Refs. 8, 47, 80—87); for further references *see* Refs. 8, 51, 79, 85, 87, 88. A clear concept would probably allow explanation and prediction of the unique combination of properties of cubic refractory compounds, i.e. their extremely high melting points and hard-

a titanium carbide TiC$_x$, after Ramqvist[91] (load 0.5 N, samples produced by arc melting) and Chermant[95] (varying load, samples produced by gas carburization, arc melting, or zone melting); *b* tantalum carbide TaC$_x$, after Ramqvist[93] (samples produced by gas carburization or hot pressing)

8 Microhardness of transition-metal carbides as function of carbon content

ness values, electrical and thermal conductivities, high strengths and elastic moduli, and high thermal stabilities. It is well established that chemical bonding can be described by three types of interatomic forces. The largest contribution to bonding is given by homopolar bonds between the metal and carbon atoms. Superimposed ionic and metallic bonding are caused by an electronic charge shift between the metal and carbon atoms and by overlapping electron functions of the metal atoms, respectively. Band structure calculations show similar and rather complicated patterns for all
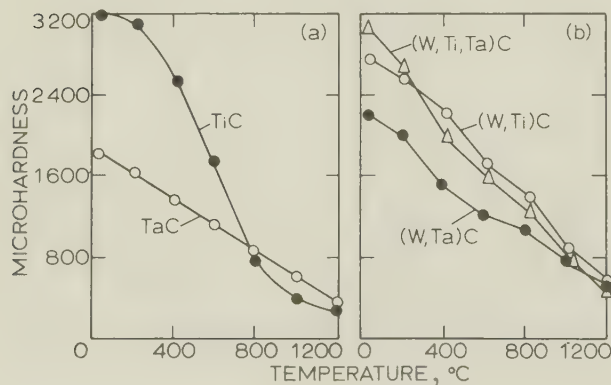
a pure carbides; *b* mixed carbides, (W, Ti)C made from 70 wt-%WC—30 wt-%TiC, (W, Ti, Ta)C made from 66 wt-%WC—27 wt-%TiC—7 wt-%TaC, and (W, Ta)C made from 10 wt-%WC—90 wt-%TaC

9 Microhardness of cubic transition-metal carbides as function of temperature; load 2.9 N, samples produced by sintering, after Miyoshi and Hara[49,50]

cubic carbides with bonding and antibonding states. The highest stability is obtained if the Fermi level lies just in the minimum between these states. Band structure calculations in the substoichiometric range are still a matter of differing opinions. Experiments, therefore, are indispensable to determine the electronic states for substoichiometric carbides, e.g. by specific heat or magnetic measurements (*see* e.g. Refs. 89, 90) and to find empirical relationships between the carbon content and the properties.

Some of these relationships are shown in Figs. 7 and 8. The lattice parameter increases with carbon content. For IVa-metal carbides the variation is relatively small (about 1.5%) and, according to Ramqvist,[91] has a maximum at a carbon/metal ratio near 0.9. This maximum corresponds to maximum stability: the highest melting temperature (*see* Fig. 2) and hardness values (*see* Fig. 8) are observed at this composition. The relatively small lattice parameters of TiC measured by Ehrlich[92] are presumably due to oxygen-forming Ti(C, O) solid solutions. The Va-metal carbides show a larger variation of lattice parameters (~10% over a smaller range of carbon/metal ratios) and a maximum hardness at a carbon/metal ratio near 0.8, i.e. somewhat above the lower limit of the stable homogeneity range. Correspondingly, minimum thermal expansion is observed at this carbon content.[96]

The temperature dependence of microhardness of TiC and TaC has been measured by Miyoshi and Hara[49, 50] and is shown in Fig. 9*a*. No information on the stoichiometry has been given by these authors but their value of room-temperature hardness of TiC seems rather high (cf Figs. 6*a* and 8*a*). The microhardness of TaC shows a gradual decrease while TiC looses its hardness quite quickly in the range between 400° and 800°C. However, at 600°C TiC is still much harder than WC and TaC.

Unfortunately, the cubic carbides are much more brittle than WC in spite of their simple crystal lattice. At room temperature, plastic deformation has not been observed. The limited toughness of the cubic carbides cancels the advantages some of them have compared with tungsten carbide (lower price, higher hardness and thermal conductivity, reduced sensitivity to carbon deficiency and temperature increase, among others). Their high mutual solubility and the high solubility of WC in most of these carbides offers additional possibilities some of which are discussed below.

Complex carbides

Complete miscibility exists between the cubic carbides of the IVa and Va metals with the exception of the pairs ZrC—VC and HfC—VC where the Hume-Rothery condition for the atomic volume is not fulfilled.[8,19] Hexagonal tungsten monocarbide, on the other hand, does not take other carbides into solid solution to any significant extent. The solubility of WC in cubic carbides ranges up to
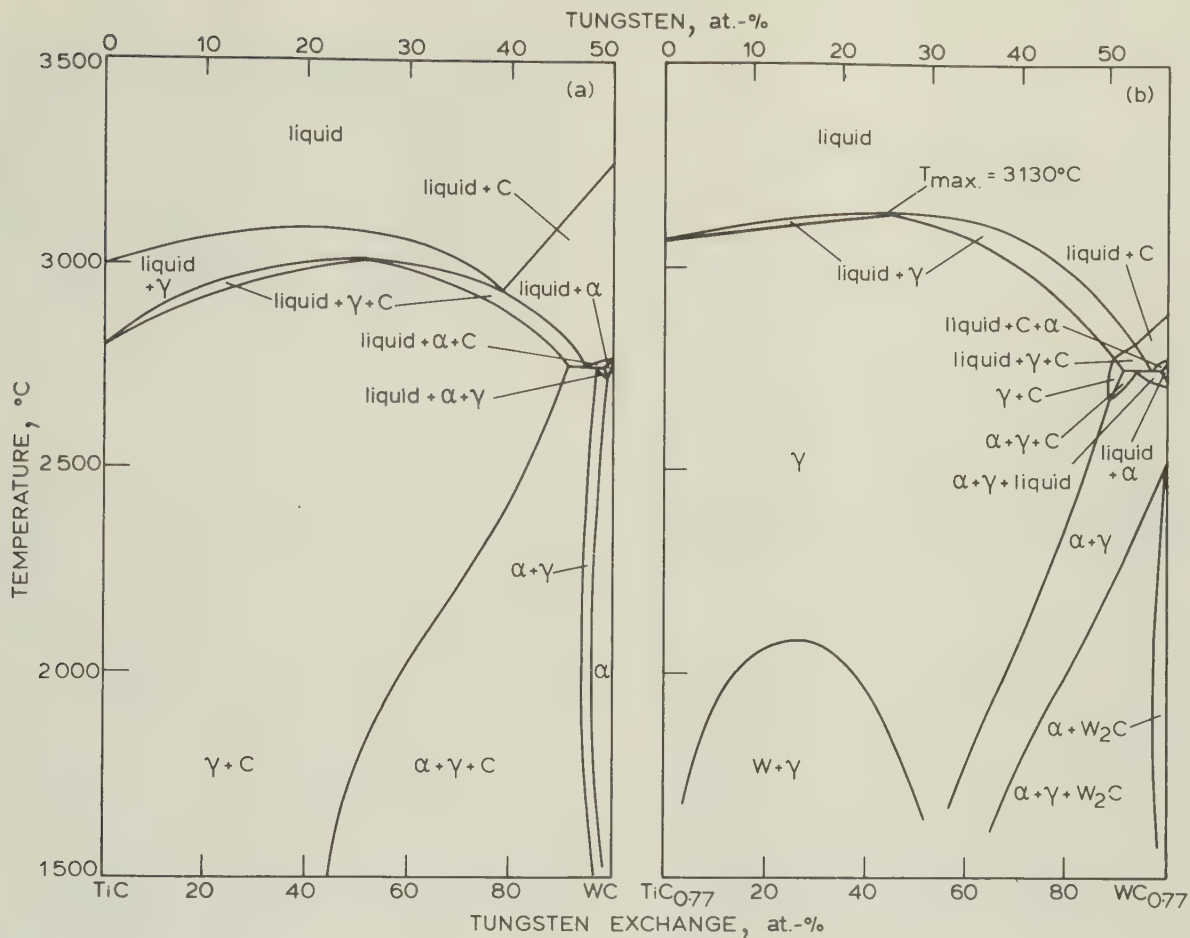
a 50 at.-%C; *b* 43.5 at.-%C

10 Temperature *v.* concentration sections in W–Ti–C system, after Rudy[24]

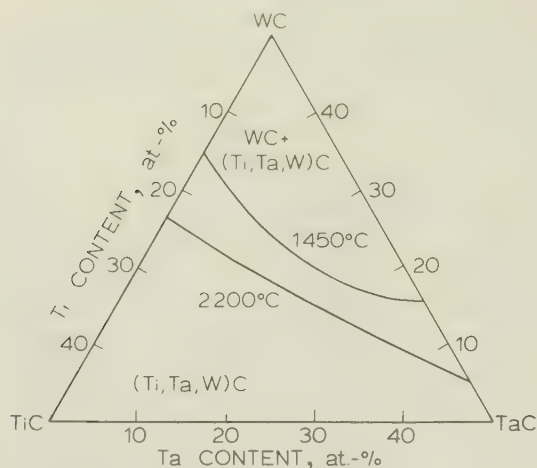70% at room temperature and up to 95% at higher temperatures.

The technically most important system in this group, W–Ti–C, has been recently re-investigated by Rudy.[24] The vertical section between the monocarbides WC and TiC (50 at.-%C) is shown in Fig. 10*a*. It is obvious that this section does not correspond to a pseudobinary system as assumed previously by Nowotny *et al.*[96] but is truly ternary. Figure 10*b* shows a vertical section at a lower carbon content (43.5 at.-%C). A point of interest in this section is the melting point maximum of the ternary solid solution at 3130°C. According to Rudy[24] there is only one other system, the V–W–C system, where a melting point maximum occurs while all the other monocarbide solutions melt incongruently. Of practical importance is the temperature-dependent precipitation of WC from the tungsten-rich cubic monocarbide solid solutions which provides a means for obtaining small particle size in cutting tools.

Other systems of interest for cemented carbides are the Ta–W–C system and the quaternary Ti–Ta–W–C system which have not been established definitely. According to Kovalski and

Umanski[97] and Nowotny *et al.*,[98] the solid solubility of TaC in WC is negligible while WC is soluble up to 15 mol.-% at 1500°C and 30 mol.-% at 2000°C in TaC. The same authors[98] investigated the 50 at.-%C section of the Ti–Ta–W–C system assuming a pseudoternary diagram. A region of homogeneous solid solutions exists in the technically important temperature range which becomes wider with increasing temperature (Fig. 11). At a higher W content practically pure WC is in equilibrium with these solid solutions. The equilibrium is very hard to achieve, even very long annealing times (of the order of days) do not usually produce a homogeneous distribution of the elements in the solid solution.[8,98]

The high-temperature hardness of some of these compositions is shown in Fig. 9*b* to be appreciably higher than that of the pure mono-carbides (Figs. 6*c* and 9*a*) at temperatures above 500°C. This was assumed to be one of the reasons for the better wear resistance of TiC–WC and TiC–WC–TaC cemented carbides in steel cutting.

A large series of complex carbides have been investigated and partially tried for potential application in hardmetals,[8,14–19,99–108] e.g. Cr_3C_2–

11 Isothermal sections in quasiternary WC—TiC—TaC phase diagram at 1450° and 2200°C

a as received; *b* after ball milling

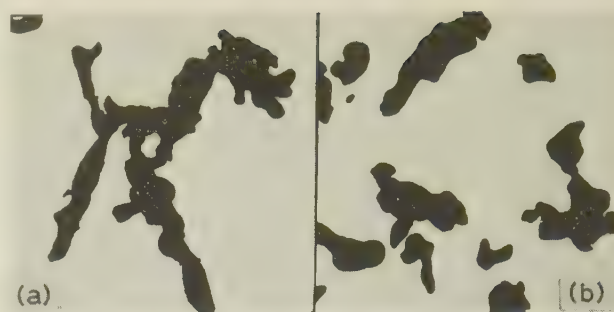**12 Typical cobalt powder used for cemented carbide production**   ×1200

TiC—WC mixtures forming a wide range of homogeneous solid solutions with a hardness maximum[99,104,105] show good sintering behaviour with a steel binder.[99] The toughness of complex carbide hardmetals seems to be insufficient however, or has not yet been studied. Although further improvements of hardmetals may be expected by the introduction of complex carbides, these will be limited to special cases. Presumably, carbonitrides will have a more pronounced impact on technical development.[9-13] For example, a series of complex compounds showing spinodal decomposition are promising for the production of high wear-performance hardmetals.[109] At present, the latter lines of development are playing only a small role technically, while coating of conventional cemented carbides with hard and wear-resistant layers of carbides, nitrides, carbonitrides, or oxides of simple or complex composition has dominated development and progress.[110-117]

STRUCTURE AND PROPERTIES OF BINDER PHASES

The metal component of cemented carbides is usually called the binder phase. The dominating metal used as a binder is cobalt, the second most used is nickel, followed by iron, while the other metals of the iron group of the periodic table have been introduced only recently in experimental alloys.

Cobalt

Cobalt is used nearly exclusively in cemented carbide production (more than 95%) because of its outstanding wetting and adhesion as well as to its advantageous mechanical properties. Cobalt powder used in cemented carbides is usually produced by hydrogen reduction; powders produced by hydrometallurgy (Sherrit-Gordon process) or atomization are used less frequently. These powders are of high purity with oxygen and

nickel as the main contaminants. A low oxygen content is advantageous but not mandatory since cobalt oxide can be reduced by hydrogen during presintering. Nickel up to several tenths of a percent in the cobalt binder does not seem to influence the final product at all. The typical particle shape is a chain-line arrangement of small rounded particles sintered during reduction (Fig. 12), the typical surface area is in the order of $1 m^2 g^{-1}$ with a crystallite size of approximately 50 nm.[118]

The initial parameters of the cobalt powders are not so important as those of the carbide powders because they are strongly altered by the milling and liquid-phase sintering process.[43,119,120] For example, the size of the cobalt grains in a sintered hardmetal is of the order of 1 mm (Refs. 4, 5, 121, 122), i.e. one grain is formed from approximately 10^9 cobalt particles of the original powder. Pure cobalt is stable in the hexagonal modification up to 417°C (Ref. 123) while a cubic modification exists at higher temperatures. In cobalt powder, typically a mixture of approximately the same amounts of the hexagonal and cubic phases is present.[118-120] During milling, the amount of hexagonal cobalt increases up to 100%.[43,119,120] In sintered alloys containing WC, the cobalt binder has a cubic lattice which cannot be transformed by annealing. The reason for this behaviour was attributed to mechanical contraints; more probable, however, it is that it is due to the stabilization of the cubic modification by dissolved tungsten and carbon.[124]

The main influence of a specific cobalt powder is exhibited during mixing and milling with the carbide constituents. Because of the wide variation of milling techniques used in industrial practice, little or only empirical information is available on the criteria for selecting an optimized cobalt powder. As stated above, this seems to be of secondary importance since all the initial properties of a cobalt powder are lost during milling and liquid-phase sintering and thus do not influence the properties of the binder phase.

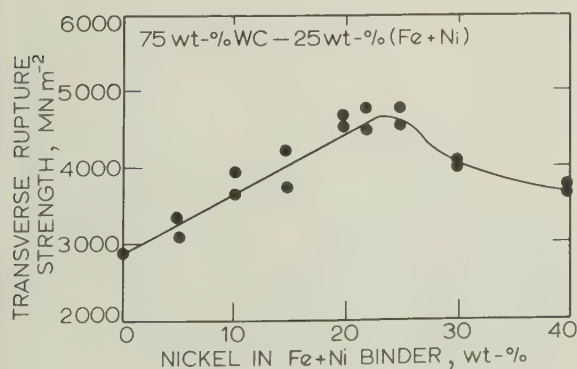### Nickel, iron, and other metals

According to earlier investigations, nickel and iron are inferior to cobalt as binder metals with

respect to the toughness of the resulting hard-metals (*see* e.g. Ref. 125). However, nickel is used now as a binder metal in technical hardmetals based on titanium carbide with molybdenum added (as metal or Mo_2C) to guarantee sufficient wetting.[106,126-129] Also, for hardmetals based on HfC and TaC, nickel seems to be the best binder metal.[102] Even for tungsten carbide, iron–nickel binders may be favourable as shown by Agte[130] and, later on, by Moskovitz *et al.*,[131] if the for-mation of η-phase is avoided by a sufficiently high carbon content. A composition of approxi-mately 75% iron and 25% nickel was shown to exhibit maximum strength values (Fig. 13), which exceed those of comparable WC–Co alloys by up to 50%.[131]

Although the possibility of martensite hard-ening was pointed out by the inventors of these alloys,[131] no systematic effect of supercooling was found. In spite of the fact that these com-positions have not yet found much technical appli-cation, the possibility of heat-treatable binders may have some future even in low binder phase hardmetals. The high binder phase Ferro-TiC materials (about 50 vol.-% steel binder, remainder TiC) point in this direction. A detailed study on WC with Fe–Ni–Co binders including heat-treat-ment effects is presently being carried out by Prakash.[132-134]

Small additions to the well known binders can have positive effects on wetting and adhesion and may be useful in technical alloys. Molybdenum in TiC–Ni alloys has been mentioned above. Chrom-ium as well as the other metals (e.g. Al or Sn) added to cobalt or nickel tend to reduce toughness at room temperature but to improve hot hardness and hot strength.[1,135]

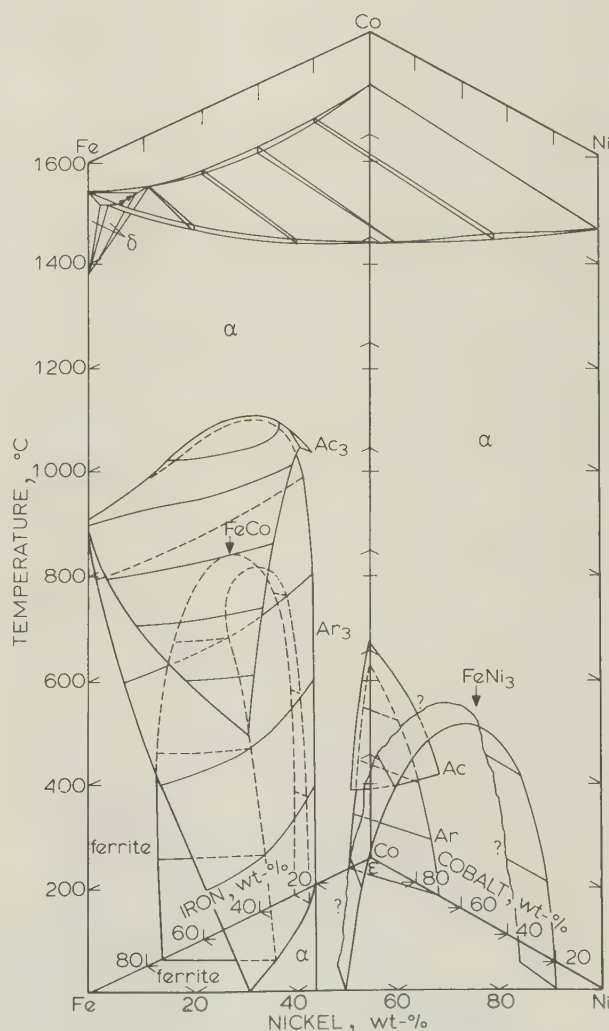Other mixed binders, mainly mixtures of cobalt and nickel have been used earlier in tech-nical alloys.[1] The phase relationships in the Fe–Ni–Co system as given in early refer-ences[136,137] are shown in Fig. 14. A more recent study[138] shows that complications due to meta-stability and sluggish transformation kinetics may

arise. This is the reason why the equilibrium relationships in the centre of the model (Fig. 14) are not complete.[137] Thus, there are still open questions on the optimum binder phase composi-tions. It must be emphasized, however, that the interaction with the carbide component will influ-ence strongly the properties of the binder phase in all cases and that final conclusions can only be drawn when the properties of the multicomponent phase diagrams (including C, W, Ti) of these metals are known (cf next section).

Platinum was used as a binder in acid-resis-tant hardmetals as early as 1951 (Ref. 1). More recently, other 'exotic' binder phases (e.g. Pd, Ru) have been investigated.[7,139] These lines seem to have little chance of leading to technically sig-nificant developments in normal cutting grades. High melting point binders, however, may be use-ful for special hot-working grades with good creep resistance at temperatures well above 1000°C.

13 Transverse rupture strength of 75 wt-% WC–25 wt-%(Fe + Ni) binder cemented car-bides, after Moskovitz *et al.*[131]

14 Co–Fe–Ni phase diagram, after Refs. 136, 137; lines labelled *Ac*$_3$ and *Ar*$_3$ refer to heating and cooling, respectively
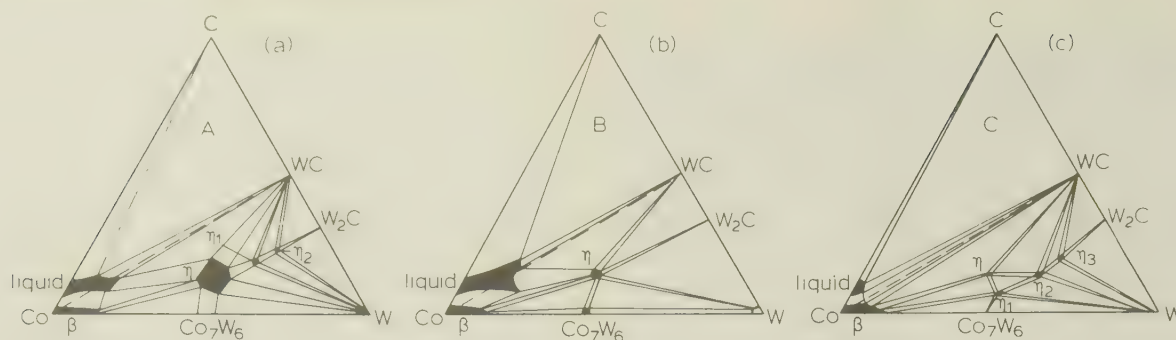
a after Rautala and Norton[141]; *b* after Grüter[142]; *c* after Pollock and Stadelmaier[143]

15 Isothermal sections of W—C—Co phase diagram at 1400°C

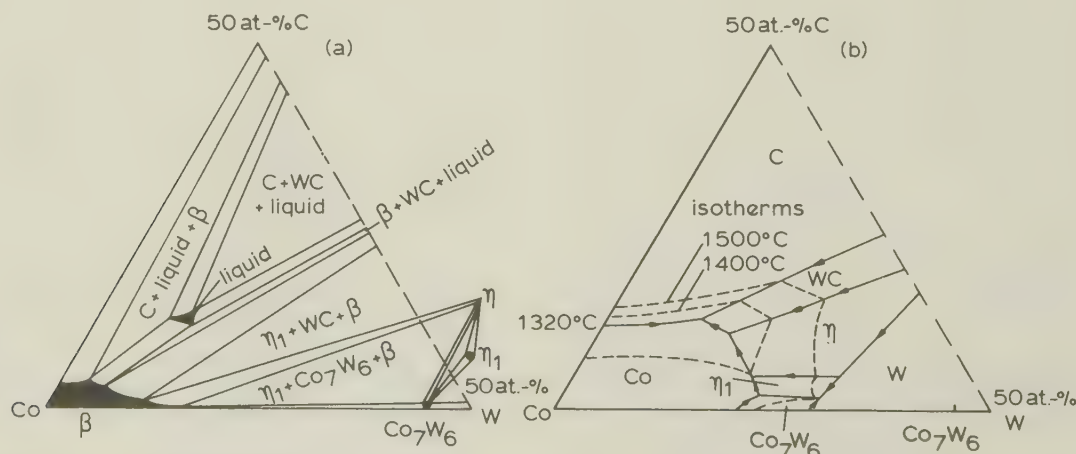## INTERACTIONS BETWEEN CARBIDES AND BINDER METALS

During the various stages of preparation of cemented carbides from powders, the carbides and the binder metal interact with each other. Interconnected networks of solid solutions (cf Fig. 1) develop and new phases (which usually are highly undesired) may be formed. In the following, the chemical and physical background of these interactions is discussed.

Carbide—binder-metal phase relationships

By far the largest part of the numerous investigations of the constitution of transition-metal—carbon—iron-metal systems is devoted to the iron corners relating to steel composition, to cobalt and nickel alloys of the superalloy type, and to Fe—Cr- and Co—Cr-based alloys used for cast wear-resisting materials.[140] On the other hand, the carbide-rich parts of most of these systems have not been established sufficiently well to give a basis for understanding the powder metallurgical behaviour of cemented carbides in detail. Even in the W—C—Co system, which has been the subject of numerous investigations[141−147] (for early literature *see also* Refs. 1, 17), there are still some open questions.

Figure 15 shows isothermal sections at 1400°C of the W—C—Co phase diagram. Rather large differences exist in the tungsten-rich corner between the various authors with three, one, and four ternary phases, respectively. The most recent investigations[145−147] do not fully agree with any of these results (Fig. 16*a*). As far as cemented carbides are concerned, all the proposed sections agree in principle. For compositions corresponding to a W/C atomic ratio close to 1, the phases WC, liquid, and β are stable. At lower carbon contents, a ternary phase η occurs. Other ternary phases or W_2C will be stable only at a much lower carbon content or at a very low cobalt content, respectively.

Figure 16*b* shows the liquidus surfaces in the cobalt-rich corner. WC precipitates primarily at compositions typical for WC—Co cemented carbides. However, η-phase will coprecipitate or occur as primary phase at lower carbon content. At W/C ratios below 1, primary carbon will precipitate and remain in equilibrium with WC and the cobalt-rich β-phase in solidified alloys. According to all the investigations cited here, the two-phase region WC + β exists only in a narrow range of carbon concentration. At room temperature the carbon concentration of WC in the two-

a isothermal section at 1260°C; *b* projection of liquidus surfaces with 1400° and 1500°C isotherms

16 Cobalt-rich part of W—C—Co phase diagram after Uhrenius *et al.*[145]
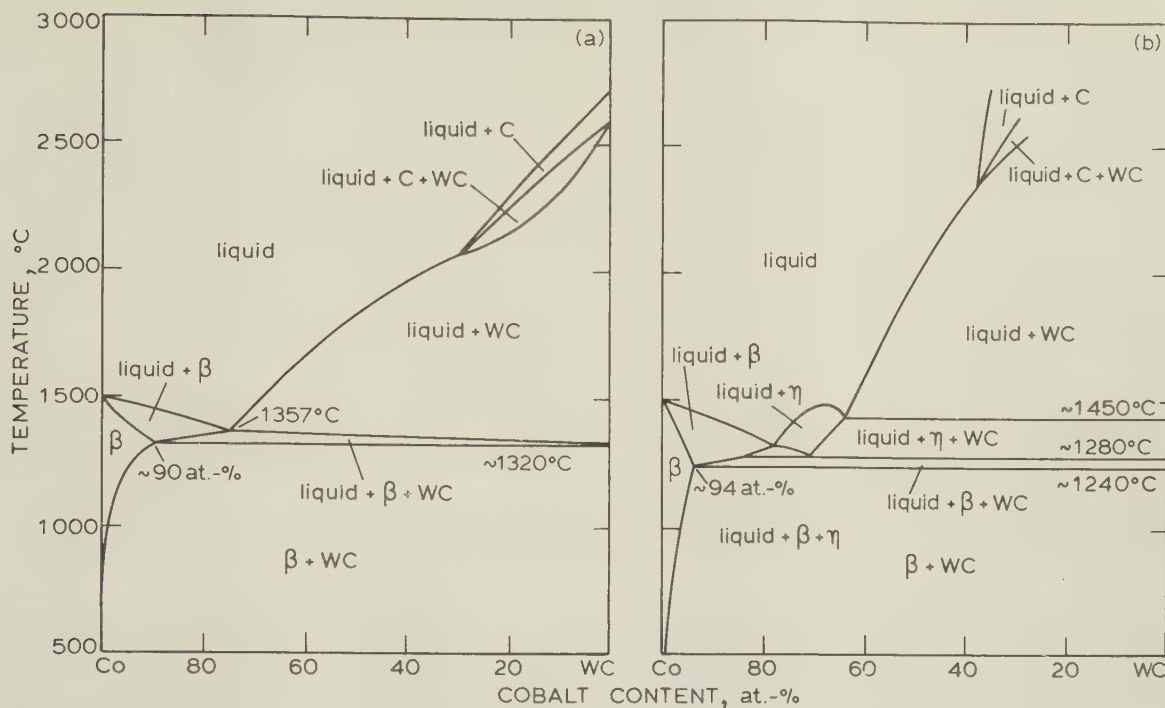
a after Rautala and Norton[141]; *b* after Grüter[142]

17 Vertical sections between stoichiometric WC and Co in WC–Co phase diagram

phase equilibrium with β was estimated previously[135] to be:

$$50 - 0.533 \text{ at.-\%Co} < \text{at.-\%C} < 50$$

or

$$6.13 - 0.0735 \text{ wt-\%Co} < \text{wt-\%C} < 6.13$$

where the left-hand limit gives the composition of WC at the boundary between the two-phase region WC + β and the three-phase region WC + β + η, while the right-hand limit is the stoichiometric composition at the limit between the two-phase region and the three-phase region WC + β + C. Vertical sections through the ternary diagram at the stoichiometric composition of WC are shown in Fig. 17. The classic proposal of Rautala and Norton (Fig. 17a) is very close to a quasibinary diagram which is very often used an an approximation in practice (e.g. Refs. 1, 43). This section, however, does not explain why η-phase may be present in cemented carbides after rapid cooling even at a relatively high carbon content. The section shown in Fig. 17b would explain these experimental findings. According to Grüter,[142] η-phase is in equilibrium with WC and liquid even at stoichiometric compositions at temperatures ranging from about 1280° to 1450°C. Since sintering of cemented carbides usually takes place in this temperature range, large η-phase regions may be retained after solidification.

The phase relationships in the W–C–Fe ternary phase diagram seem to be very similar to those described above for the W–C–Co system. The isothermal sections at 1000°C established by Pollock and Stadelmaier[143] agree very closely for both systems. Deviating phase relationships were found by Bergström[148] which correspond more closely to the W–C–Co system given by Johansson and Uhrenius.[147] These authors investigated also the compositions of the η-phases in the four-component system W–C–Fe–Cr. No quaternary carbides were found and a 8 at.-% solubility of chromium in the η-phase M_6C was established.

Quasibinary sections were assumed to exist in the systems Ti–C–Ni and Ti–C–Co between the monocarbide and the binder phase.[1,149,150] Bäckerud *et al.*[151] gave a review on these and other earlier studies and established liquidus surfaces for the nickel- and cobalt-rich corners of these systems, *see* Fig. 18. An isothermal section in the Ti–C–Co system was reported by Kossowsky and Harvey.[152] Because of the wide homogeneity range of TiC, other carbide phases do not occur in hardmetals made from these systems even at larger deviations from the stoichiometric carbon content.

Literature on other phase diagrams in the region of hardmetal compositions is scarce or non-existent. This fact is amazing and can only be explained by the fact that commercial hardmetals are developed on an empirical rather than on a scientific basis. It is hoped that the work of the Swedish school[144,147,151] will be extended and that the tedious and often not conclusive experimental methods can be circumvented by a calculation of phase relationships from
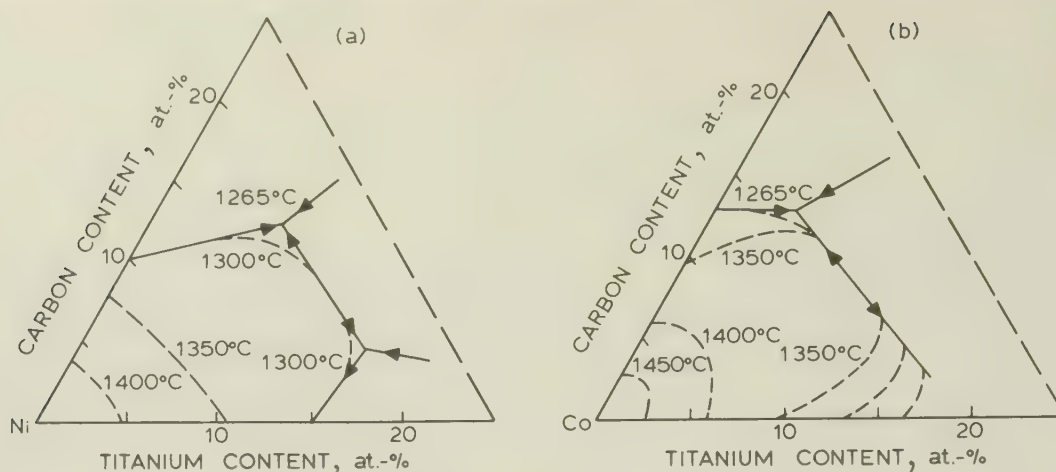
a Ti—C—Ni; *b* Ti—C—Co

18   Projections of liquidus surfaces in binder-phase-rich corners of Ti—C—Ni and Ti—C—Co phase diagrams after Bäckerud *et al.*[151]

thermodynamic data. With the equilibrium phase relationships (especially those in the W—Ti—C—Co, W—Ta—Ti—C—Co, and Ti—Mo—C—Ni systems) known, hardmetal production would be easier to control and development of new and improved compositions should be possible.

Solubility of carbides in binder metals

Another problematic feature of the interaction of carbides with the iron-group metals is their solubility. It is well established that cobalt and nickel do not dissolve in the monocarbides. The solubility of carbides in the binder is appreciable and plays an important role in hardmetal production since it controls the properties of the binder phase. In earlier work, only the solubility of stoichiometric carbides was considered. Although partially out of date, the results of Edwards and Raine[153] are given in Table 3. It is interesting to note that the solubilities in cobalt and nickel throughout are higher than those in iron. This was assumed to be the reason for the preferential use of these two metals as a binder, and the exceptionally high solubility of WC in Co was taken as a major cause for the good toughness of these composites. More recent as well as earlier work (*see* Ref. 154), however, showed that the solubility of WC in Co is lower, and a value of about 9.5 wt-%WC is accepted at present according to

a solution of 3 at.-%W (8.9 wt-%) and 3 at.-%C (0.6 wt-%) at the temperature of the non-variant ternary equilibrium (about 1250°C). These values agree with the phase diagram shown in Fig. 17*b* and constitute the solubilities at the high carbon limit. There seems to exist a reciprocal relationship between the dissolved tungsten [W], and the dissolved carbon [C], corresponding to an equilibrium constant of the reaction $W + C = WC$, i.e. $[W] \cdot [C] = $ constant. At the low carbon limit of 0.7 at.-% (0.12 wt-%) the solubility of tungsten in solid cobalt amounts to about 10 at.-% (26 wt-%) (Ref. 154) suggesting an equilibrium constant $[W] \cdot [C]$ of about 7×10^{-4}, while a value for $[W] \cdot [C]$ of 9×10^{-4} is obtained for the upper carbon limit (*see* above). Thus, for precipitation-free cobalt alloys, the solubility limits of tungsten and carbide may be represented by $[W] \cdot [C] = 8 \times 10^{-4}$ within the limits cited above where [W] and [C] are given in atomic fractions.

In W—C—Co alloys with WC precipitates or additional phases (η or Co_3W), the amount of tungsten dissolved in cobalt is greatly reduced, especially during slow cooling. In addition to the cooling rate and the carbon content, the tungsten content in WC—Co hard alloys is determined by the size of the cobalt domains, i.e. by the amount and the size of the WC crystals. These effects have been studied extensively during the last few

Table 3   Solid solubilities (in wt-%) of some carbides in binder metals at 1250°C (Ref. 153)

Binder	WC	TiC	TiC/WC 1:1	TaC	NbC	VC*	Mo$_2$C	Cr$_3$C$_2$
Co	22	1	2	3	5	6	13	12
Ni	12	5	5	5	3	7	8	12
Fe	7	0.5	0.5	0.5	1	3	5	8

*V$_4$C$_3$ in the original paper.

years[121],[154-163] since they suggest an influence of heat treatment on the properties of technical hardmetals. The possibility of influencing the properties of WC–Co alloys by annealing was pointed out in earlier work[164-167] but was not well understood then. More work seems necessary to utilize these findings in industrial practice, especially in terms of the isothermal temperature–time–transformation diagrams of Jonsson and Aronsson.[121] These diagrams indicate that W–C–Co alloys show a precipitation behaviour corresponding to that of steels and, thus, the use of heat treatments for WC–Co hardmetals similar to those used for commercial steels or high-binder TiC–Fe alloys seems feasible.

Little is known about the composition of binder phases in WC–Co alloys containing additional carbides or metals. To explain grain-growth inhibition it was speculated that carbides of the group Va metals reduce the solubility of WC in Co.[168] This hypothesis, however, could not be confirmed in a later investigation.[169] Nickel additions were shown to increase the solubility of tungsten in the binder.[170] The influence of the carbide content on the binder-phase composition of a (W, Ti, Ta, Nb)C–Co alloy was investigated recently by Johnson[171] and shown to follow similar lines to WC–Co alloys.

The problem in determining binder-phase compositions is the small size of the metal domains compared to the resolution of the available detectors (microprobe) and the difficulty of detecting carbon with the high degree of accuracy needed. Magnetic saturation measurements have proven very useful in controlling the amount of tungsten dissolved in the binder,[124],[163],[172] and therefore can be used advantageously as a non-destructive method in quality control. The exact characterization of the binder-phase composition is of the utmost practical importance since the controlled variation of the binder phase by small additions and careful control of the carbon content seems to have the greatest potential for improvements of technical hardmetals.

Wetting

Many of the important processes during hardmetal production are related to the energy of interfaces, i.e. the energy of the carbide-phase/binder-metal interface and its relation to the grain-boundary energy of the carbide. Solid-state and liquid-phase sintering, formation of microstructure, and mechanical properties depend critically on these physical quantities.

The most obvious effect of the interfacial energy is its effect on the wetting behaviour of the liquid binder and the solid carbide. By analyzing the shape of a liquid drop in contact with a flat carbide surface, precise values of interfacial energies can be obtained if the surface energies of the carbide and the melt are known. This 'sessile drop method' and the Young equation relating the interfacial and the surface energies

to the wetting angle are well known (*see* e.g. Refs. 173, 174) and need not to be discussed here. The most important quantity for characterizing the wetting behaviour is the work of adhesion W_A, which is experimentally determined from the wetting angle θ according to the equation

$$W_A = \gamma(1 + \cos\theta)$$

where γ is the surface energy of the melt.

Detailed studies on the wetting of carbides by liquid metals (preferentially copper) have been carried out by Ramqvist,[47],[175] who also gives a review of earlier work, and by Goretzki and co-workers.[79],[87] Studies of the wetting behaviour of metals not used as binder metals are not only of academic interest. Hardmetal inserts are often fixed to steel by soldering and good wetting and adhesion are essential. The results of wetting studies are wide spread in the literature. Since the relationships between wetting angle and work of adhesion, on the one hand, and sintering and mechanical behaviour, on the other, are not quantitatively established, there is no need to report these values here.

Samsonov[176],[177] first tried to give an explanation of the good wetting properties of the iron-group metals by relating this to their functioning as electron acceptors owing to an unfilled d-band. Ramqvist[47] showed that a linear relationship exists between the work of adhesion and the energy shift of the $C1s$ electrons measured by ESCA (Fig. 19a). Since an increasing energy shift indicates increasing ionic bonding, Ramqvist relates wetting to the stability of the carbides: the more stable the carbide, the smaller its affinity to metals and, consequently, the smaller the wetting tendency. Although assuming covalent bonding of the carbides rather than ionic, Goretzki and co-workers[79] arrived at the same conclusion by varing the stoichiometry and the metal in carbides of the group IVa and Va metals. Subsequently, Goretzki and Scheuermann[87] showed a linear relationship between the work of adhesion and the free-electron concentration (Fig. 19b) and assumed a metallic bonding at the metal/carbide interface. These attempts to elucidate the atomistic nature of wetting have not led as yet to a consistent theoretical approach to the wetting behaviour of carbides. It seems safe to conclude, however, that a strong chemical bond exists at the interface between carbides and the iron-group metals.

Chemical bonding is especially favourable in the case of tungsten carbide and cobalt. This results in a very low interfacial energy for this combination,[178] nearly perfect wetting, and a very good adhesion in the solid state. The wetting angle of cobalt on tungsten is zero and spreading occurs readily, independently of the degree of vacuum or the type of inert atmosphere used. In earlier work (*see* Refs. 44, 135) it was assumed that a thin cobalt layer exists between the tungsten crystals in sintered WC–Co alloys. No direct
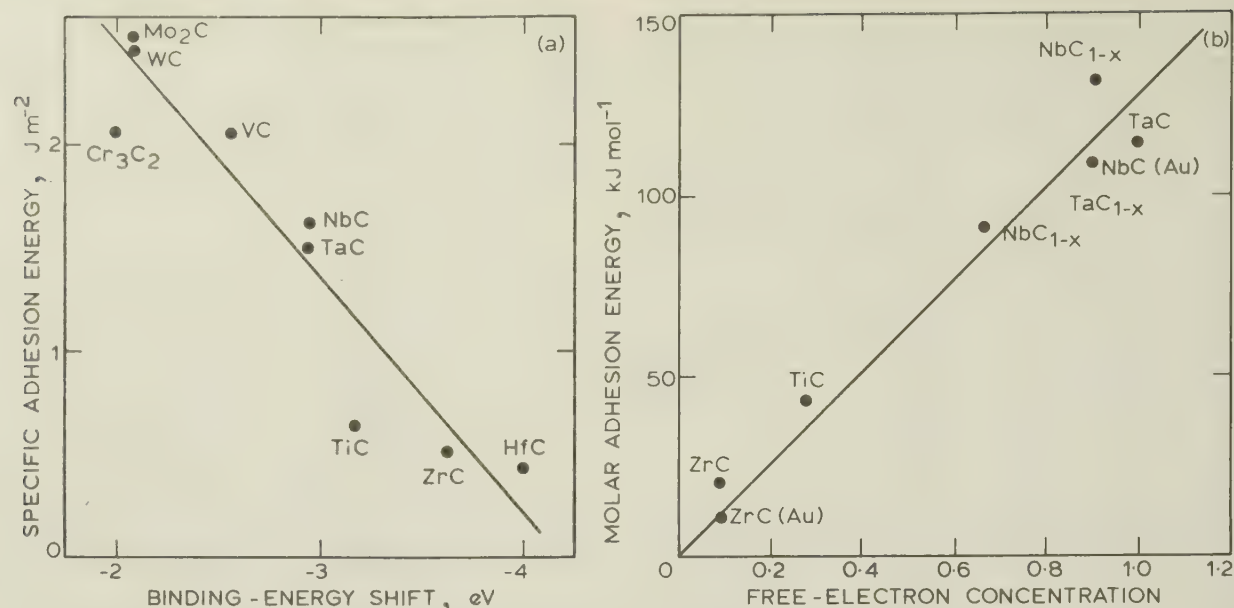
a correlation with ionicity (shift in the binding energy of *C1s* electrons), after Ramqvist[47]; *b* correlation with free-electron concentration, after Goretzki and Scheuermann[87]

19 Correlations between work of adhesion for copper (or gold, when indicated) and electronic properties of various carbides

proof (e.g. by microprobe analysis) is available for this hypothesis, which is based on the assumption that perfect wetting exists, or on the experimental observation that WC—Co alloys deform plastically and disintegrate if the cobalt phase is removed. As discussed earlier in detail by Exner and Fischmeister[44] it is now generally accepted (*see also* the section on 'Contiguity'), that during sintering grain boundaries develop between the carbide crystals (presumably enriched with cobalt) demonstrating that the dihedral angle is not zero. Because of the high anisotropy of the surface energy of WC, equilibrium dihedral angles are not established.

Other carbide—binder-metal combinations are less favourable as far as wetting is concerned. While cobalt penetrates easily into hot-pressed tungsten carbide, copper or tin do not[179] though copper wets tungsten carbide well enough to allow infiltration of pressed powder compacts.[180] Sufficient wetting for cemented carbide production was observed for tungsten carbide and essentially all metals of the iron group studied, i.e. WC—Fe, WC—Ni, WC—Fe—Ni, and WC—Fe—Ni—Co,[132-134] WC—Ru and WC—Pd,[139] or WC—Pt.[1]

Technically more important is the wetting behaviour of titanium carbide, which has recently been reviewed by Attlegård.[181] As mentioned above, wetting in the TiC—Ni system is improved by addition of Mo or Mo_2C. A recent study[182] has confirmed the strong influence of the ambient atmosphere in this system. At 1400°C, wetting angles of about 18° and 42° were observed in vacuum and dry hydrogen (oxygen partial pressure 10^{-9} Pa), respectively. At a lower oxygen

pressure (10^{-11} Pa), no equilibrium was obtained and the lowest angle observed was 12°. It is interesting to note that presaturation of the nickel melt with titanium and carbon did not have any influence on wetting and spreading. At low oxygen pressures, nickel penetrates into the grain boundaries of polycrystalline titanium carbide[182] but, as in WC—Co, grain boundaries form again during sintering. Sufficient wetting was observed also in other TiC-based hardmetals, for example, in TiC—Ru.[183]

In conclusion, wetting is not usually a limiting factor in the production of technical hardmetals. Spreading of metals of the iron group occurs readily and grain boundaries between or in carbide-powder particles are penetrated in most cases indicating perfect wetting. The formation of contacts between the carbide crystals during sintering shows that the grain boundaries in pure carbides differ from those in cemented carbides in that the grain-boundary energy is reduced (presumably by taking up metal atoms) and wetting becomes incomplete. Difficulties arising during sintering owing to insufficient wetting may be overcome by additions changing the electronic interchange between the carbide and the binder metal or by adjusting the carbon (or oxygen) potential of the ambient atmosphere.

Residual stresses

During cooling from sintering temperature, thermal stresses develop in hardmetal compositions because of the pronounced difference in the thermal-expansion coefficients of transition-metal carbides and binder metals. For example,
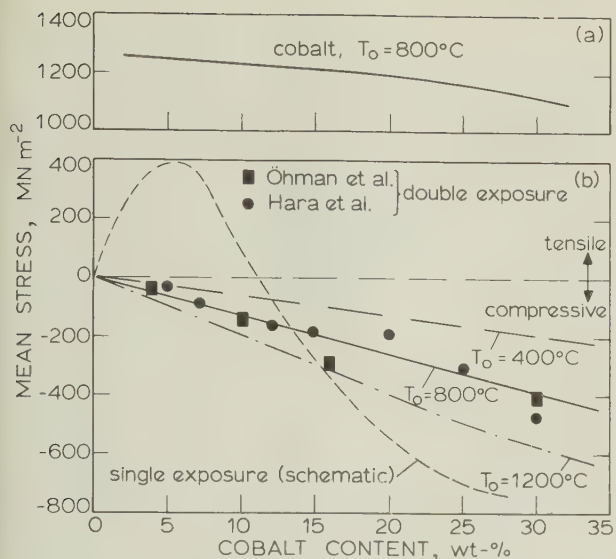
the thermal contraction of cobalt is approximately three times that of WC. A series of X-ray investigations have been carried out together with theoretical considerations to establish the sign and the magnitude of these stresses in WC—Co alloys,[76,184-192] while only a few papers have been published on thermal stresses of other carbide—metal combinations, e.g. Refs. 193, 194.

In early work[185,186] using the single-exposure X-ray technique, tensile stresses were assumed to exist in the carbide phase of low-cobalt alloys (Fig. 20) and a theoretical model was established to explain this trend.[186] It was first pointed out by Amberg[192] and confirmed by X-ray investigations using the double-exposure technique[76,187-191] that thermal stresses are compressive in the carbide phase of WC—Co alloys at all compositions (Fig. 20) and that the results obtained by the single-exposure technique are in error.

Theoretical considerations predict an approximately linear increase of the compressive stresses in WC with increasing cobalt content.[76,192] For the temperature at which thermal stresses are first set up during cooling a temperature range between $T_0 = 400°$ and $1200°C$ was discussed in earlier work,[76,184,192] where T_0 is the temperature above which the binder phase is too soft to carry any load and residual stresses disappear by local creep. In Fig. 20, curves are

a tensile stresses in Co, calculated; *b* stresses in WC, single-exposure results, schematic corresponding to results from Gurland[185] and Bernard[186]; data points double-exposure results from Öhman *et al.*[76] and Hara *et al.*[190,191]; theoretical curves after Amberg[192] and Öhmann *et al.*[76] (for 800°C recalculated)

20 Thermal stresses in WC—Co alloys as function of cobalt content
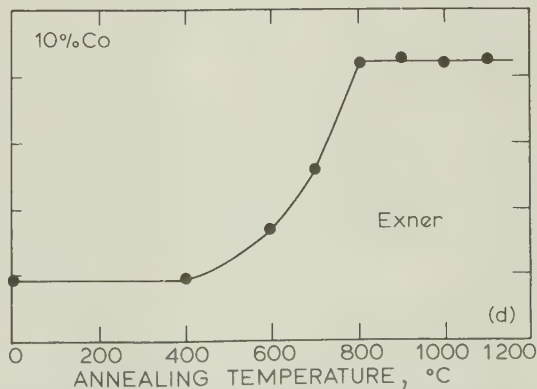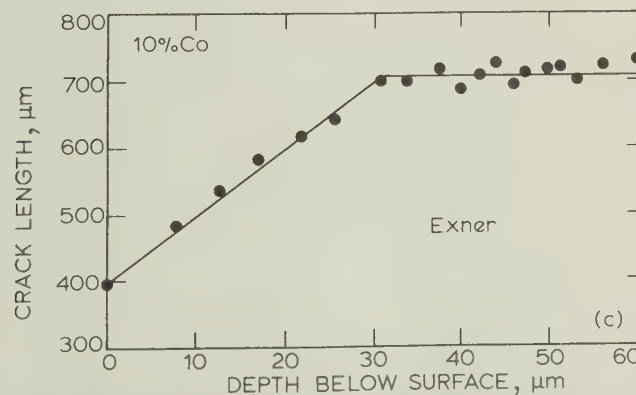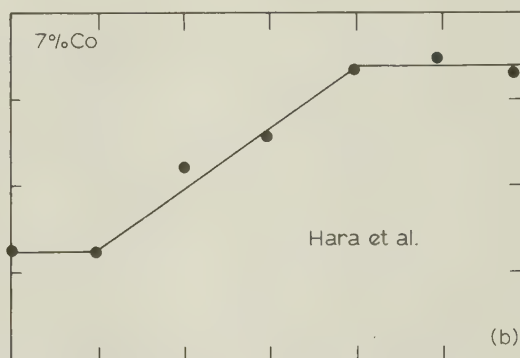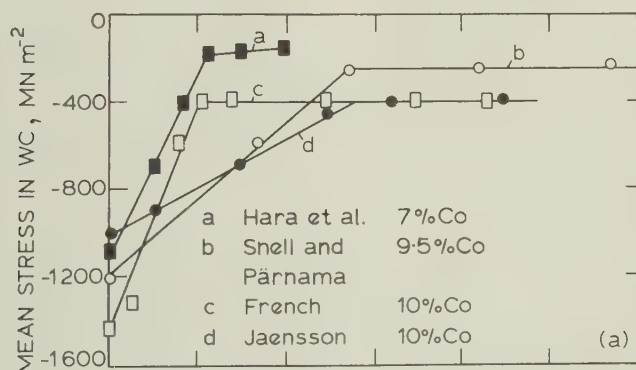

21 Residual stresses and crack length at Vickers indentations as *a, c* function of depth below a ground surface and *b, d* annealing temperature, after Hara *et al.*,[190,191] Snell and Pärnama,[189] French,[196] Jaensson,[197] and Exner[195]

given for $T_0 = 400°$, $800°$, and $1200°C$. Although local creep is obviously not completely independent of cooling conditions and cobalt content[189] T_0 is now well established to be of the order of $800°C$. In annealing experiments it has been shown by direct[190,191] as well as by indirect[195] evidence that residual stresses introduced by mechanical deformation persist during a heat treatment below $800°C$, while at $800°C$ and at higher temperatures a reproducible stress level is obtained which corresponds to the deformation-free state (*see* Fig. 21). In addition, the excellent agreement of data from Swedish[76] and Japanese[190,191] workers with theoretical predictions for $T_0 = 800°C$ is striking (Fig. 20). Although deviating results have been reported (e.g. Ref. 188), the linear dependence $\sigma = 13X_{Co}$ between the compressive stress σ (in MN m^{-2}) in the carbide phase and the cobalt content X_{Co} (in wt-%) can serve as a practical guide line for thermal stresses in WC—Co alloys in the range of technical compositions.

To establish stress equilibrium, the tensile stress in the binder phase must be very high. Theoretical estimates show that the stress level is above 1000 MN m^{-2} over the entire range of technical compositions of WC—Co alloys. Because of the combination of increasing stress in the carbide phase with larger load-carrying cross-section of the cobalt-binder phase, the stress in the cobalt phase decreases only slightly with increasing cobalt content (Fig. 20). Because of the rather low Bragg angle and the low intensity of suitable X-ray reflections, the direct determination of the stress in the cobalt phase is difficult and inaccurate. An attempt has been made by Snell and Pärnama[189] for a 9.5 wt-% cobalt alloy, but this measurement (compressive stress of 150 MN m^{-2}) does not seem compatible with the value of compressive stress (250 MN m^{-2}) found in the carbide.

The stress pattern introduced during cooling can be modified by a mechanical treatment. Experiments aiming to change the stress distribution in the bulk of the sample by small plastic deformations have been carried out.[198] No conclusive results were obtained as far as the effect on residual stresses and bulk properties is concerned. Although some influence of residual stresses on yield and fracture strength has been assumed occasionally (*see* Refs. 60, 198, 199), no significant changes in hardness or transverse rupture strength were observed after plastic deformation. On the other hand, the length of cracks at the edges of Vickers hardness indentations reacts very sensitively to this mechanical treatment.[198] As shown in Fig. 22a the cracks in the direction of compression become much larger than those in the direction normal to the load indicating a highly anisotropic stress pattern while cracks of approximately equal length are obtained in samples as received after sintering (Fig. 22b).

A very pronounced influence on the residual stress pattern in WC—Co alloys is exhibited by

(a)

(b)
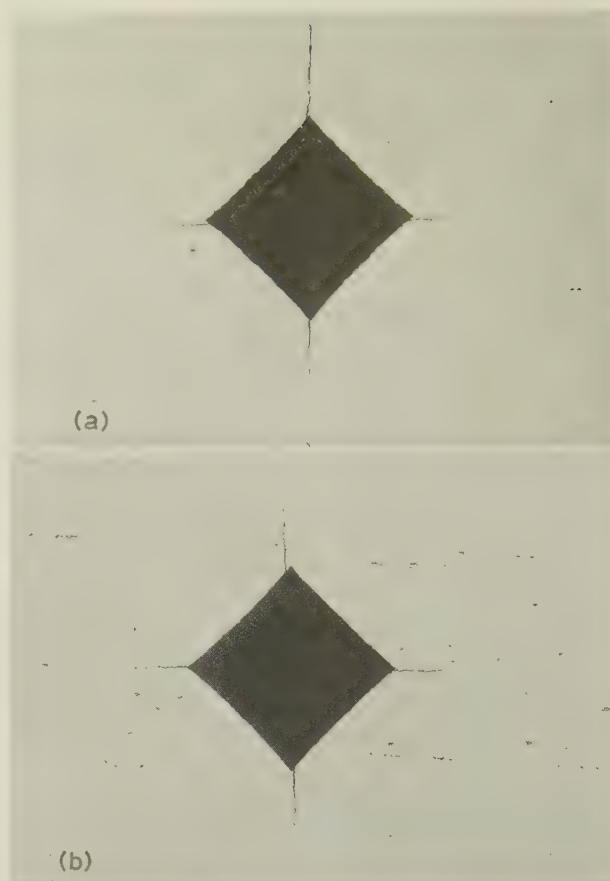
a sample deformed in compression by 0.2% in vertical direction, note marked extension cracks in this direction; *b* underformed sample

22 Cracks at Vickers hardness indentations, after Exner[198]   ×100

grinding. Compressive stresses are introduced in regions near to the surface which, depending on the cobalt content and the severity of grinding, increase the stress level in the carbide phase up to 1500 MN m^{-2} (Refs. 76, 189—191, 195—197, 200). In the cobalt phase, the tensile stresses are reduced or converted to compressive stresses. Stress equilibrium is established by tensile stresses at some depth below the surface.[195,197] By polishing, the deformed layer can be removed gradually until the stress reaches a constant level corresponding to the equilibrium thermal stresses. In this way it was shown that grinding stresses extend to a depth ranging from 10 to 100 μm, which depended on the cobalt content and the grinding conditions.[189—191,195—197] As mentioned above, the original stress state can be established also by annealing at temperatures above $800°C$. Some of these results are shown in Fig. 21. Again, hardness is not influenced by this deformation but the crack length depends sensitively on the stress state at the surface. Since cracking occurs due to tensile stresses, compressive stresses at the surface reduce the crack

length (Fig. 21) as was pointed out by Exner[195] and confirmed by other authors.[190,191,196] The expected influence of surface stresses on the transverse rupture strength has not been demonstrated conclusively as yet. This effect has been discussed recently by Suzuki and Hayashi.[200]

The change of stresses in the carbide phase of WC—Co alloys during bending was studied by Jaensson[197] and by Kraus.[201] The most interesting findings of these investigations are the hysteresis in the stress—strain curves and the deviations between the nominal loading stress and the local stress in the carbide phase.

Although the amount of knowledge presented above is rather limited it seems obvious that residual stresses must be considered as an important parameter in understanding the properties of cemented carbides.

MICROSTRUCTURAL ASPECTS

Following the pioneering work of Gurland,[202,203] methods for the quantitative evaluation of the microstructure of cemented carbides have been worked out by numerous authors.[43,44,204-222] Reviews containing additional references have been presented earlier.[44,211] In most of these papers, the influence of preparation conditions on the geometrical configuration of the microstructure has been studied too. The relationships between microstructural parameters and mechanical or magnetic properties have been extensively investigated for WC—Co alloys (e.g. Refs. 43, 135, 202, 203, 211—213), for early references *see* Exner and Gurland[135] and Fischmeister and Exner.[213] However, relatively little information is available for other cemented carbide compositions.[139,181,205,208-210,220] Some important parameters of the microstructure will be discussed briefly below.

Size and size distribution

The sizes of the carbide crystals and of the cobalt regions (frequently called 'carbide grain size' and 'cobalt layer thickness', respectively) depend upon the size and the size distribution of the starting powders, the milling and sintering conditions, and the composition of the alloy. It is interesting to note that a high carbon content generally promotes the growth of tungsten carbide while it reduces that of titanium carbide and that small changes in composition have a strong influence on the coarsening of the microstructure during sintering (*see* e.g. Refs. 169, 220). Apart from these effects, the influence of the preparation parameters mentioned above is relatively well understood.

The shape of the size distribution of carbide grains in sintered cemented carbides assumes a fairly constant shape for a given alloy composition. The size distribution of WC grains in cobalt can be very closely approximated by a log—normal distribution.[43,44,221] Extremely large grains occur occasionally in the microstructure of WC—Co

alloys, most often owing to discontinuous grain growth during oversintering, transformation of η-phase, or during hot pressing causing deviations from the smooth size-distribution curves (*see* e.g. Ref. 44). In practice, discontinuous grain growth is supressed by additions of TaC as mentioned above. After very long annealing times, the size distribution of VC grains in 40 vol.-% binder phase (Co or Ni) alloys coincides with the stationary size distributions predicted theoretically for reaction-controlled Ostwald ripening.[220,222] These types of distributions (log—normal and stationary reaction-controlled) have been claimed also to describe the size distribution of WC, TiC, or VC crystals in low-cobalt alloys[208,209] but pronounced deviations have been observed also. The varying shape of the carbide crystals makes it difficult and in most cases impossible to apply the available procedures for establishing the true spatial size distribution from cross-sections[223] and great care must be taken in using these procedures for cemented carbides.[222,224]

The distribution of the binder phase is related to the spacing between the carbide crystals. Since a continuous cobalt network with fluctuating width of the branches exists, rather than well defined cobalt layers, the term cobalt layer thickness is misleading. The mean linear intercept in the binder phase (also called 'mean free path') is used widely to describe the distribution of the cobalt phase in WC—Co and (Ti, W)C—Co alloys. Rather than the 'nominal mean free path' assuming cobalt layers between all carbide grains defined by Gurland and Bardzil,[202] the 'true mean linear intercept' taking visible cobalt regions only into account[44,204,213] should be used.[135] This parameter is inversely proportional to the specific surface of the binder phase (carbide/binder interface per unit volume of binder) and thus represents the most important single parameter for characterization of the geometry of the binder phase. The proportionality between the specific surface of the binder phase and the coercive force (*see* e.g. Refs. 124, 210, 211, 213) can be used for non-destructive control of microstructural parameters.

Little is known about the variation of the cross-sections of the cobalt network. The only quantitative information available to this author shows that a log—normal distribution fits the experimental results on the linear intercept size distribution of the cobalt phase in WC—12 wt-%Co alloys with varying carbon content.[124] According to this investigation, the width of the size distribution exhibits a measurable influence on the properties.

Contiguity

One of the important aspects of the microstructure of cemented carbides is the degree to which a continuous skeleton of the carbide phase exists in hardmetal compositions used in practice. According to the generally adopted proposal by Gurland,[203]
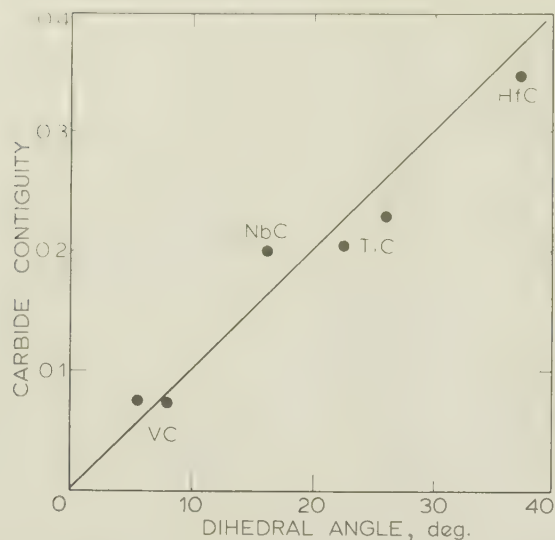
**23 Contiguity of cemented carbides (grain-bound-
ary area/total interface area) with dihedral
angle for various carbides with 20 vol.-%Co
binder phase, after Warren and Waldron[139]**

the degree of skeleton formation can be quantita-
tively defined by the ratio of grain-boundary area
to total interface of the carbide grains, and is
called 'contiguity'. This parameter can be deter-
mined easily by quantitative metallography (*see*
e.g. Refs. 203, 204, 211).

For cubic carbides forming rounded grains,
contiguity varies linearly with the dihedral angle
which the binder phase forms at carbide grain
boundaries[139] as shown in Fig. 23. Tungsten car-
bide (contiguity of about 0.4 at 20 vol.-% Co,
Ref. 44) does not fit this scheme if a dihedral angle
near zero degrees is assumed. Since the angu-
larity of the carbide grains does not allow an
equilibrium dihedral angle to be established, an
effective value of about 40° can be used. For TaC,
forming habit planes and cubic crystals instead of
equilibrium dihedral angles, the contiguity of an
alloy with 20 vol.-% Co is also about 0.4 (Ref. 139).
These results indicate that contiguity is governed
by geometrical conditions rather than by inter-
facial energy equilibrium in these cases.

As expected, contiguity decreases with in-
creasing amount of binder (Fig. 24). The amount of
binder phase at which the carbide phase becomes
discontinuous was a matter of controversy (*see*
e.g. Ref. 225). In early work it was assumed that
the WC skeleton breaks down at a binder-phase
content of as little as 10 vol.-% (Ref. 203). In the
opinion of the author of the present review, a con-
tinuous carbide phase exists throughout the range
of most commercial hardmetal compositions up to
a high binder content (well above 30 vol.-%).

Increasing sintering time and sintering tem-
perature tend to decrease contiguity indicating
that grain-boundary surface decreases more
rapidly than cobalt/carbide interface area. At

constant sintering conditions, contiguity is inde-
pendent of carbide crystal size. This is interest-
ing since it implies that cemented carbides of
constant composition show geometrical similarity
in their microstructure, i.e. one parameter (mean
carbide grain size or mean linear cobalt intercept)
is sufficient to describe quantitatively the micro-
structure of WC–Co alloys. This fact should be
kept in mind when the source of relationships
between microstructural parameters and proper-
ties is considered. Even for varying binder-phase
content and sintering conditions, the mean linear
intercept in the binder phase L_{Co}, the mean linear
size of the carbide grains L_{WC}, and contiguity C
are not independent parameters. The following
equation holds[213]

$$L_{WC} = L_{Co} (1 - C)(1 - f)/f$$

where f is the volume fraction of the binder phase.
Therefore, it is not surprising that close correla-
tions have been found between properties, e.g.
transverse rupture strength, and all parameters
involved in the above equation (*see* e.g. Refs. 202,
211–214).

Shape and homogeneity of the carbide crystals

As discussed above, the prismatic shape of the
WC crystals is related to their crystal structure.
In low binder-phase alloys the grains cannot
assume their ideal equilibrium shape but are
truncated owing to interference with other crys-
tals during growth. However, in fully sintered
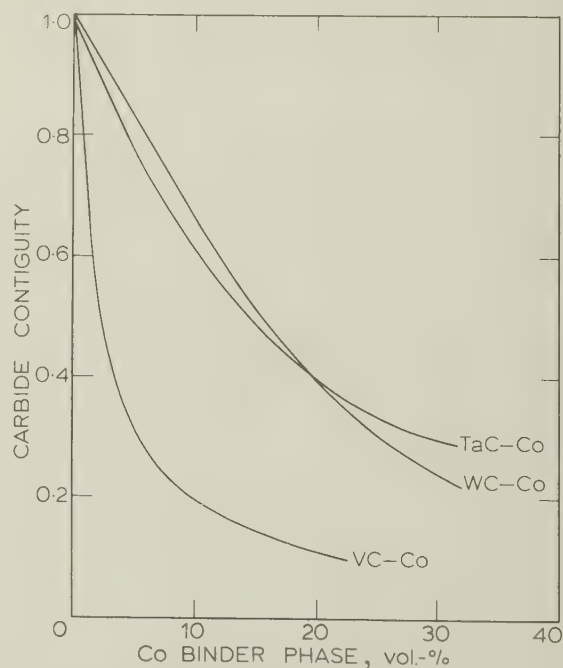
**24 Contiguity of cemented carbides as function of
cobalt content; WC after Exner and Fisch-
meister[44] and TaC and VC after Warren and
Waldron[139]**

alloys, WC crystals show plane interfaces with the binder phase independently of which binder metal is used and which additional carbides are present. According to Gurland,[225] rounded WC grains may occur in a transition stage when η-phase is carburized to give WC and Co. Deviations from the prismatic shape can also be observed during coalescence, i.e. when several small grains grow together and the resulting crystal has not yet assumed its equilibrium shape. It must be emphasized, however, that the rounded appearance of small grains is usually owing to lack of optical resolution or over-etching.[43,44] Because of the small homogeneity range of WC, inhomogeneities in WC crystals could not be detected by the available measuring techniques.

Tantalum carbide shows plane interfaces in a cobalt or a nickel matrix if its carbon content is near stoichiometry. The grains appearing in metallographic cross-sections can be interpreted as intersections of cubes with slightly rounded corners and edges[139,220,222] and TaC particles produced by the menstruum technique are nearly ideal cubes. Substoichiometric TaC_{1-x}, on the other hand, forms rounded crystals (*see* e.g. Ref. 102). Even more sensitive to variations in carbon content (and oxygen impurities) is the shape of the TiC grains in nickel.[220] When the carbon content is very high, the shape of the powder particles is retained and irregular grains are observed even after prolonged sintering. Reducing the carbon content by Ti or TiO_2 additions of the order of 2 wt-% produces rounded grains and with higher additions angular idiomorphic grains of cubic TiC are obtained. In commercial alloys TiC usually appears rounded (*see* e.g. Refs. 226, 227) indicating that a carbon content appreciably below stoichiometry exists.

Both TaC and TiC crystals which have grown during sintering show pronounced coring owing to a inhomogeneous carbon content. The original particles show up as light areas inside a darker etching core of precipitated material. Rounded and inhomogeneous grains of the cubic phase are also observed in WC–TiC–TaC–Co alloys (cf Fig. 1b). The mechanism of this coring has been studied extensively but is still not completely understood (for references *see* Rüdiger and Exner[4]). Small additions of cubic carbides to WC–Co alloys form 'dotted' microstructures, i.e. the additions show up as dark spots after etching (*see* e.g. Ref. 169).

The other pure cubic carbides as well as carbide mixed crystals also form rounded grains becoming angular or cubic depending upon their composition, the binder metal used, and the sintering conditions where coarsening takes place (*see* e.g. Ref. 205). Vanadium carbide seems to be the only example for which angular grains have not been observed, nearly spherical crystals were obtained even at high carbon levels[139,205,220,222] as well as in the menstruum process.[228] This indicates a very low degree of crystal anisotropy.

It is interesting also that coring was not observed in VC crystals in spite of its large range of homogeneity and pronounced coarsening.

Porosity and other defects

Although modern cemented carbide production is directed towards minimizing the flaw content in the sintered parts, pores and other defects (cracks or inclusions) are usually present to some extent in the microstructure. The size and the shape of these flaws are related to composition and preparation conditions. For example, a low carbon content and insufficient mixing makes the alloy prone to pore formation during sintering. Other reasons for pores are entrapped gases or an uneven density distribution after pressing. In a number of recent papers,[229–235] the causes and effects of porosity in cemented carbides have been discussed in detail. There is little doubt that strength is related intimately to these flaws in the way predicted by fracture-toughness arguments.

Isostatic hot pressing is used to reduce porosity as far as possible[162,229–233] especially in cases where porosity not only reduces toughness but also is detrimental for the application of finished parts owing to other reasons (e.g. surface smoothness of cold rolls). However, flaws cannot be completely eliminated by this technique either. Figure 25 shows the pore size distribution in high-quality WC–Co grades.

Because of the extremely low frequency of observation in metallographic cross-sections (typically 10^{-4} mm^{-2}, *see* Fig. 25), large pores and defects are not typical features of the microstructure. This makes quality control difficult. Comparison of unetched cross-sections with standard charts still prevails for assessment of
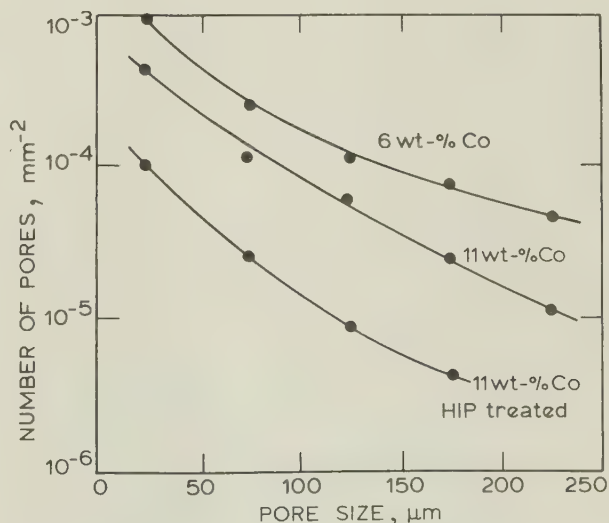
25 Pore size distribution in sintered and isostatic hot-pressed WC–Co alloys, after Amberg and Doxner[229]; cumulative number of pores (larger than size indicated on the abscissa) is plotted

porosity.[229,236] However, statistical methods have been developed for the more accurate investigations[229] necessary in research work as well as for modern cemented carbides which are produced under extreme cleanliness. From Fig. 25 it can be seen that the extrapolation of metallographic results is problematic. X-ray, γ-ray, ultrasonic, and other techniques are used to obtain more information.[229]

REFERENCES

1. R. Kieffer and F. Benesovsky: 'Hartmetalle'; 1965, Wien, New York, Springer-Verlag.
2. K. J. A. Brookes: 'World directory and handbook of hardmetals', 2 ed.; 1979, London, Engineer's Digest.
3. R. Kieffer and P. Ettmayer: *Chem.-Ing.-Tech.*, 1974, **46**, 843.
4. O. Rüdiger and H. E. Exner: 'Powder metallurgy—promises and problems', 122; 1975, Paris, Matériaux et Techniques.
5. O. Rüdiger and H. E. Exner: *Powder Metall. Int.*, 1976, **8**, 7.
6. E. Lardner: *Powder Metall.*, 1978, **21**, 65.
7. M. B. Waldron: *Neue Hütte*, 1978, **23**, 317.
8. R. Kieffer and F. Benesovsky: 'Hartstoffe'; 1963, Wien, New York, Springer-Verlag.
9. R. Kieffer, P. Ettmayer, and M. Freudhofmeier: *Metall*, 1971, **25**, 1335.
10. R. Kieffer, P. Ettmayer, and M. Freudhofmeier: 'Modern developments in powder metallurgy', Vol. 5, (ed. H. H. Hausner), 201; 1971, New York, Plenum Press.
11. I. I. Bilyk: *Sov. Powder Metall. Met. Ceram.*, 1972, (6), 466.
12. R. Kieffer, H. Nowotny, P. Ettmayer, and G. Dufek: *Metall*, 1972, **26**, 701.
13. H. Grewe: 'Handbuch der Keramik'; 1976, Freiburg, Verlag Schmid.
14. E. K. Storms: 'The refractory carbides'; 1976, New York, London, Academic Press.
15. L. Toth: 'Transition metal carbides and nitrides'; 1971, New York, Academic Press.
16. T. J. Kossolapova: 'Carbides, properties, production and applications'; 1971, New York, Plenum Press.
17. G. V. Samsonov: 'High temperature materials, properties index'; 1964, New York, Plenum Press.
18. T. B. Schaffer: 'High temperature materials, materials index'; 1964, New York, Plenum Press.
19. F. Benesovsky: 'Ullmanns Encyklopädie der Technischen Chemie', Vol. 9, 122; 1975, Weinheim, Verlag Chemie.
20. K. Becker: 'Hochschmelzende Hartstoffe und ihre technische Anwendung'; 1933, Berlin, Verlag Chemie.
21. M. Hansen and K. Anderko: 'Constitution of binary alloys'; 1958, New York, McGraw-Hill.
22. D. K. Gupta and L. L. Seigle: *Metall. Trans.*, 1975, **6A**, 1939.
23. R. V. Sara: *J. Am. Ceram. Soc.*, 1965, **48**, 251

24. E. Rudy: *J. Less-Common Met.*, 1973, **33**, 245.
25. K. Kirner: cited in Ref. 8, p. 190.
26. A. Hara and M. Miyake: *Planseeber. Pulvermetall.*, 1970, **18**, 91.
27. A. Hara and M. Miyake: *Nippon Kinzoku Gakkai-Si*, 1969, **33**, 1323.
28. F. Kölbl; *Planseeber. Pulvermetall.*, 1971, **19**, 18.
29. L. Ramqvist: 'Modern developments in powder metallurgy', Vol. 4, (ed. H. H. Hausner), 75; 1971, New York, London, Plenum Press.
30. E. Neuenschwander: *J. Less-Common Met.*, 1966, **11**, 365.
31. R. Kieffer and H. Rassaerts: *Int. J. Powder Metall.*, 1966, **2**, (2), 15.
32. R. Kieffer, H. Rassaerts, and D. Schob: *Monatsh. Chem.*, 1965, **96**, 685.
33. R. Kieffer and G. Jangg: *Powder Metall. Int.*, 1972, **4**, 191.
34. R. Kieffer and G. Jangg: *ibid.*, 1973, **5**, 25.
35. A. Westgren and G. Phragmén: *Z. anorg. allg. Chem.*, 1926, **156**, 27.
36. E. Parthé and V. Sadagopan: *Monatsh. Chem.*, 1962, **93**, 263.
37. D. N. French and D. A. Thomas: 'Anisotropy in single-crystal refractory compounds', (eds. F. V. Vahldiek and J. Mersol), Vol. 1, 55; 1968, New York, Plenum Press.
38. H. Pfau and W. Rix: *Z. Metallkd.*, 1954, **45**, 116.
39. J. Corteville and L. Pons: *CR Hebd. Séances Acad. Sci.*, 1963, **257**, 1915; 1965, **260**, 2773, 4477.
40. T. Takahashi and E. J. Freise: *Philos. Mag.*, 1965, **12**, (115), 1.
41. D. N. French and D. A. Thomas: *Int. J. Powder Metall.*, 1967, **3**, (3), 7.
42. M. Malli and E. Hillnhagen: *Prakt. Metallogr.*, 1967, **4**, 16.
43. H. E. Exner: 'Struktur und Eigenschaften der Hartlegierung WC10%Co', Jernkontoret Technical Report JK U8 64—20, 1964, Stockholm. (Copies available from the author.)
44. H. E. Exner and H. F. Fischmeister: *Arch. Eisenhüttenwes.*, 1966, **37**, 417.
45. H. Krainer: *ibid.*, 1950, **21**, 119.
46. J. Gurland: *Trans. AIME*, 1957, **209**, 512.
47. L. Ramqvist: *Jernkontorets Ann.*, 1969, **153**, 159.
48. D. N. French and D. A. Thomas: *Trans. AIME*, 1965, **233**, 950.
49. A. Miyoshi and A. Hara: *Sumitomo Electr. Tech. Rev.*, 1966, (7), 68.
50. A. Miyoshi and A. Hara: *J. Jpn Soc. Powder Metall.*, 1965, **12**, 78.
51. G. M. Schwab and A. Krebs: *Planseeber. Pulvermetall.*, 1971, **19**, 91.
52. F. Benesovsky and A. Ihrenberger, *Prakt. Metallogr.*, 1966, **3**, 126.
53. J. Corteville: *Rev. Inst. Franc. Petr.*, 1966, **21**, 1355.
54. L. Pons: 'Anisotropy in single-crystal refractory compounds', (eds. F. V. Vahldiek and J. Mersol), Vol. 2, 393; 1968, New York, Plenum Press.

55. O. Rüdiger: 'Proc. 2nd conf. on powder metallurgy in Poland', Krakow, 1967, 199; Warsaw, Polska Akademia Nauk.
56. S. Bartolucci and H. H. Schlösslin: *Acta Metall.*, 1966, **14**, 337.
57. S. Bartolucci-Luyckx: PhD thesis, University of Witwatersrand, Johannesburg, 1967.
58. S. Bartolucci-Luyckx: *Acta Metall.*, 1970, **18**, 233; 1975, **23**, 109.
59. A. Myoshi, A. Hara, and Y. Sugimoto: *Plan- seeber. Pulvermetall.*, 1967, **15**, 187.
60. R. Arndt: *Z. Metallkd.*, 1972, **63**, 274.
61. J. Burbach: 'Proc. 2nd European symp. on powder metallurgy', Paper 7. 13; 1968, Stutt- gart, Ausschuß für Pulvermetallurgie.
62. J. L. Chermant, A. Jost, and F. Osterstock: *Proc. Br. Ceram. Soc.*, 1975, **25**, 197.
63. E. Kohlhaas, O. Jung, and A. Fischer: *Prakt. Metallogr.*, 1972, **9**, 243.
64. E. A. Almond and B. Roebuck: *Met. Technol.*, 1978, **5**, 92.
65. A. Hara, T. Nishikawa, and T. Nishimoto: *J. Jpn Soc. Powder Metall.*, 1970, **16**, 310.
66. A. Hara, T. Nishikawa, and T. Nishimoto: *Sumitomo Electr. Tech. Rev.*, 1970, **14**, 106.
67. T. Johannesson and B. Lehtinen: *Philos. Mag.*, 1971, 24, (191), 1079.
68. T. Johannesson and B. Lehtinen: 'On the plasticity of tungsten carbide', Report IM—910, 1972, Stockholm, Swedish Institute for Metals Research.
69. G. Persson: 'Proc. 6th Plansee seminar on high temperature materials', (ed. F. Bene- sovsky), 672; 1969, Reutte, Metallwerke Plansee.
70. J. L. Chermant, M. Coster, G. Hautier, and P. Schaufelberger: *Powder Metall.*, 1974, **17**, 85.
71. M. Contre, M. Coster, A. Dechanvres, and L. Pons: *Powder Metall. Int.*, 1971, **3**, 33.
72. V. A. Ivensen, N. Eiduk, and L. Kh. Pivovarov: *Sov. Powder Metall. Met. Ceram.*, 1964, (4), 300.
73. J. G. Baldoni and W. S. Williams: *Ceram. Bull.*, 1978, **57**, 1100.
74. G. S. Kreimer and N. A. Alekseeva: *Sov. Phys. Met. Metallogr.*, 1961, **13**, 114.
75. H. Doi, Y. Fujiiwara, K. Miyake, and Y. Oosawa: *Metall. Trans.*, 1970, **1**, 1417.
76. S. Öhman, E. Pärnama, and S. Palmqvist: *Jernkontorets Ann.*, 1967, **151**, 126.
77. O. Rüdiger and A. Winkelmann: *Tech. Mitt. Krupp*, 1960, **18**, 19.
78. H. Pfau and W. Rix: *Z. Metallkd.*, 1952, **43**, 440.
79. H. Goretzki, H. E. Exner, and W. Scheuer- mann: 'Modern developments in powder metallurgy', Vol. 4, (ed. H. H. Hausner), 327; 1971, New York, Plenum Press.
80. H. Bilz: *Z. Phys.*, 1958, **153**, 338.
81. V. Ern and A. C. Switendick: *Phys. Rev.*, 1965, **137A**, 1927.
82. R. G. Lye and E. M. Logothetis: *ibid.*, 1966, **147**, 622.
83. H. Goretzki: *Keram. Z.*, 1969, **21**, 238.
84. H. J. Weiss: 'Proc. 3rd powder metallurgy conf. in Poland', Zakopane, 1971, 89; Warsaw, Polska Akademia Nauk.
85. A. Merz: *Neue Hütte*, 1972, **17**, 7.
86. H. J. Weiss: 'Proc. 5th powder metallurgy conf. in the DDR', Vol. 2, Paper 25; 1973, Dresden, Akademie der Wissenschaft der DDR.
87. H. Goretzki and W. Scheuermann: 'Preprints of 7th Plansee seminar', Vol. 4, Paper 50; 1971, Reutte, Planseewerke.
88. P. Costa: 'Anisotropy in single-crystal re- fractory compounds', (eds. F. W. Vahldiek and J. Mersol), Vol. 1, 151; 1968, New York, Plenum Press.
89. H. Bittner and H. Goretzki: *Monatsh. Chem.*, 1962, **93**, 5.
90. G. V. Samsonov and V. Ya. Naumenko: *Teplofiz. Vys. Temp.*, 1970, **7**, 1093.
91. L. Ramqvist: *Jernkontorets Ann.*, 1968, **152**, 517.
92. P. Ehrlich: *Z. anorg. Chem.*, 1949, **259**, 1.
93. L. Ramqvist: *Jernkontorets Ann.*, 1968, **152**, 465.
94. R. Lesser and G. Brauer: *Z. Metallkd.*, 1958, **49**, 622.
95. J. L. Chermant: *Rev. Int. Hautes Temp. Réfract.*, 1969, **6**, 299.
96. H. Nowotny, R. Parthé, R. Kieffer, and F. Benesovsky: *Z. Metallkd.*, 1954, **45**, 97.
97. A. E. Kovalski and J. S. Umanski: *Z. Fiz. Chim.*, 1946, **20**, 773.
98. H. Nowotny, R. Kieffer, and O. Knotek: *Berg Hüttenmänn. Monatsh.*, 1951, **96**, 6.
99. L. Stojanov and H. E. Exner: *Z. Metallkd.*, 1978, **69**, 60.
100. H. Holleck and F. Thümmler: *Planseeber. Pulvermetall.*, 1975, **23**, 175.
101. H. Holleck and F. Thümmler: 'Proc. 4th round table conf. on sintering', (ed. D. P. Uskovic), 159; 1977, Belgrade, International Institute for the Science of Sintering.
102. H. Holleck and F. Thümmler (eds.): Reports of the Kernforschungszentrum, Karlsruhe; KFK— Ext. 6/73—3, 1973; KFK—Ext. 6/7—2, 1974; KFK—Ext. 6/74—5, 1974; KFK—Ext. 6/78—1, 1978. (Copies available from Librarian, Kernforschungszentrum, Karlsruhe.)
103. H. Nowotny: *Angew. Chem.*, 1972, **84**, 973.
104. O. Rüdiger: *Metall*, 1953, **7**, 967.
105. O. Rüdiger: *Tech. Mitt. Krupp*, 1954, **12**, 22.
106. E. Rudy: US Patent No. 3 690 962, 1972.
107. R. Kieffer, G. Trabesinger, and N. Reiter: *Planseeber. Pulvermetall.*, 1969, **17**, 25.
108. M. Brunn and V. S. Stubican: *J. Am. Ceram. Soc.*, 1974, **57**, 117.
109. E. Rudy, S. Worchester, and W. Elkington: *High Temp.—High Pressure*, 1974, **6**, 497.
110. R. Kieffer, D. Fister, and E. Heidler: *Metall*, 1972, **26**, 128.
111. G. Schumacher: *Tech. Z. prakt. Metallbearbeit.*, 1969, **63**, 275.
112. K. Naik: *Planseeber. Pulvermetall.*, 1977, **25**, 32.

113. R. Kieffer, D. Fister, H. Schoof, and K. Maurer: *Powder Metall. Int.*, 1973, **5**, 188.
114. W. Schintlmeister and O. Pacher: *Metall*, 1974, **28**, 690.
115. J. G. Siranov and N. J. Razkazov; 'Proc. 6th int. powder metallurgy conf. in the DDR', Vol. 2, Paper 41; 1977, Dresden, Akademie der Wissenschaft der DDR.
116. W. Schedler: *Maschinenmarkt,* 1976, **82**, 1967.
117. W. Schintlmeister, O. Pacher, and K. Pfaffinger: *J. Electrochem. Soc.*, 1976, **123**, 924.
118. M. H. Tikkanen, A. Taskinen, and P. Taskinen: *Powder Metall.*, 1975, **18**, 259.
119. J. Hinnüber, O. Rüdiger, and W. Kinna: *ibid.*, 1961, (8), 1.
120. H. F. Fischmeister and H. E. Exner: *Planseeber. Pulvermetall.*, 1965, **13**, 17.
121. H. Jonsson and B. Aronsson: *J. Inst. Met.*, 1969, **97**, 281.
122. J. Wilbrand and U. Wieland: *Int. J. Powder Metall.*, 1972, **8**, 89.
123. J. B. Hess and C. S. Barrett: *Trans. AIME*, 1952, **194**, 645.
124. J. Freytag: PhD thesis, Universität Stuttgart, 1977. (Copies available from the author of this review.)
125. P. Schwarzkopf and R. Kieffer: 'Cemented carbides', 188; 1960, New York, Macmillan.
126. M. Humenik and N. M. Parikh: *J. Am. Ceram. Soc.*, 1956, **39**, 60.
127. D. Moskowitz and M. Humenik: 'Modern developments in powder metallurgy', Vol. 3, (ed. H. H. Hausner), 83; 1966, New York, Plenum Press.
128. W. Fairhurst: *Metallurgia*, 1968, **77**, 145.
129. K. Nishigaki, T. Ohnishi, T. Shiokawa, and H. Doi: 'Modern developments in powder metallurgy', Vol. 8, (eds. H. H. Hausner and W. S. Smith), 627; 1974, Princeton, NJ, Metal Powder Industry Federation.
130. C. Agte: *Neue Hütte*, 1957, **2**, 537.
131. D. Moskovitz, M. J. Ford, and M. Humenik: 'Modern developments in powder metallurgy', Vol. 5, (ed. H. H. Hausner), 225; 1971; New York, London, Plenum Press.
132. L. Prakash: 'Contemporary inorganic materials', (eds. G. Petzow and W. J. Huppmann), 158; 1978, Stuttgart, Riederer-Verlag.
133. L. Prakash: Ref. 102, KFK—6/78—1, 1978, pp. 66, 87.
134. R. Oberacker and L. Prakash: Ref. 102, KFK—6/78—1, 1978, pp. 57, 78.
135. H. E. Exner and J. Gurland: *Powder Metall.*, 1970, **13**, 13.
136. W. Gürtler (ed.): 'Constitution of ternary metallic systems'; 1956, Berlin, Martin Wienke KG.
137. 'Cobalt monograph'; 1960, Bruxelles, Centre d'Information du Cobalt.
138. C. Servant, G. Cizeron, and P. Lacombe: *J. Iron Steel Inst.*, 1973, **211**, 75.
139. R. Warren and M. B. Waldron: *Powder Metall.*, 1972, **15**, 166.
140. O. Knotek, E. Lugscheider, and H. Eschnauer: 'Hartlegierungen für den Verschleißschutz'; 1975, Düsseldorf, Verlag Stahleisen.
141. P. Rautala and T. Norton: 'Proc. 1st Plansee seminar', 303; 1952, Reutte, Planseewerke.
142. H. Grüter: Thesis, Universität Münster, 1959.
143. C. B. Pollock and H. H. Stadelmaier: *Metall. Trans.*, 1970, **1**, 767.
144. B. Haglund and B. Uhrenius: *Met. Progr.*, 1976, **110**, (8), 40.
145. B. Uhrenius, B. Carlson, and T. Franzén: *Scand. J. Metall.*, 1976, **5**, 49.
146. A. Harsta, T. Johansson, S. Rundqvist, and J. O. Thomas: *Acta Chem. Scand.*, 1977, **31A**, 260.
147. T. Johansson and B. Uhrenius: *Met. Sci.*, 1978, **12**, 83.
148. M. Bergström: *Mater. Sci. Eng.*, 1977, **27**, 257, 271.
149. V. N. Eremenko, V. M. Polyakova, and Z. A. Golubenko: *Akad. Nauk Ukr. SSR*, 1959, (3), 62.
150. L. D. Brownley and T. Raine: cited in Ref. 1.
151. L. Bäckerud, B. Carlsson, R. Oskarsson, and M. Mikus: *Scand. J. Metall.*, 1974, **3**, 725.
152. R. Kossowsky and F. J. Harvey: *Metall. Trans.*, 1974, **5**, 790.
153. R. Edwards and T. Raine: 'Proc. 1st Plansee seminar', 232; 1952, Reutte, Planseewerke.
154. A. Hoffmann and R. Mohs: *Metall*, 1974, **28**, 661.
155. M. Komač: 'Contemporary inorganic materials 1976', (eds. D. Kolar and M. Komač), 8; 1976, Ljubljana, Josef Stefan Inst.
156. H. Jonsson: *Powder Metall.*, 1972, **15**, 1.
157. O. Rüdiger, D. Hirschfeld, A. Hoffmann, J. Kolaska, G. Ostermann, and J. Willbrand: *Tech. Mitt. Krupp,* 1971, **29**, 1.
158. O. Rüdiger, D. Hirschfeld, A. Hoffmann, J. Kolaska, G. Ostermann, and J. Willbrand: *Int. J. Powder Metall.*, 1971, **7**, (1), 29.
159. A. Hoffmann: *Metall*, 1971, **25**, 493.
160. K. Voigt and U. Voigt: *Neue Hütte,* 1974, **19**, 103.
161. J. Vavrda: *ibid.*, 1978, **23**, 381.
162. H. Grewe and J. Kolaska: *Metall*, 1978, **32**, 989.
163. D. L. Tillwick and I. Joffe: *Scr. Metall.*, 1973, **5**, 479.
164. V. I. Tumanov, V. F. Funke, Z. S. Trukhanova, T. A. Novikova, and K. F. Kuznetsova: *Sov. Powder Metall.*, 1964, (2), 131.
165. V. I. Tumanov, V. F. Funke, Z. S. Trukhanova, T. A. Novika, and K. F. Kuznetsova: *Poroshk. Metall.*, 1964, (2), 57.
166. A. A. Betser and J. Gurland: 'Some effects of temperature and heat-treatment on the strength of sintered WC—Co alloys', Publication 66—MD—17; 1966, ASME.
167. H. Suzuki, M. Sugiyama and T. Umeda: *Nippon Kinzoku Gakkai-Si*, 1964, **28**, 287.
168. S. R. Palmqvist: 'Symposium on powder metallurgy 1954', 305; 1956, London, The Iron and Steel Institute.
169. H. Grewe, H. E. Exner, and P. Walter: *Z. Metallkd.*, 1973, **64**, 85.

170. H. Suzuki and T. Yamamoto: *J. Jpn Soc. Powder Metall.*, 1968, **15**, (2), 20.

171. H. Johnson: 'Preprints 5th European symp. on powder metallurgy', Vol. 2, 69; 1978, Stockholm, Jernkontoret.

172. J. Freytag, P. Walter, and H. E. Exner: *Z. Metallkd.*, 1978, **69**, 546.

173. T. J. Whalen and M. Humenik: 'Progress in powder metallurgy', Vol. 18, 85; 1962, Princeton, NJ, Metal Powder Industry Federation.

174. J. F. Paddy (ed.): 'Wetting, spreading and adhesion; 1978, London, New York, San Francisco, Academic Press.

175. L. Ramqvist: *Int. J. Powder Metall.*, 1965, **1**, (4), 2.

176. G. V. Samsonov: *Sov. Powder Metall. Met. Ceram.*, 1968, (71), 874.

177. G. V. Samsonov: 'Proc. 6th Plansee seminar on high temperature materials', (ed. F. Benesovsky), 10; 1969, Reutte, Metallwerke Plansee.

178. H. E. Exner and H. Fischmeister: *Z. Metallkd.*, 1966, **57**, 187.

179. A. F. Lisovkii: *Sov. Powder Metall. Met. Ceram.*, 1977, (176), 611.

180. G. E. Spriggs and P. Walter: personal communication, 1978.

181. M. Attlegård: Literaturstudie IM—1004; 1974, Stockholm, Institutet för Metallforskning.

182. K. Tähtinen and M. H. Tikkanen: 'Preprints 5th European symp. on powder metallurgy', Vol. 2, 255; 1978, Stockholm, Jernkontoret.

183. R. Warren and M. B. Waldron: *Powder Metall. Int.*, 1975, **7**, 18.

184. H. Pfau and W. Rix: *Z. Metallkd.*, 1952, **43**, 440.

185. J. Gurland: *Trans. ASM*, 1958, **50**, 1063.

186. R. Bernard: *Jernkontorets Ann.*, 1963, **147**, 22.

187. S. Palqvist: *Verkstäderna*, 1963, **59**, 187.

188. D. N. French: *J. Am. Ceram. Soc.*, 1969, **52**, 267, 271.

189. P. O. Snell and E. Pärnama: *Planseeber. Pulvermetall.*, 1973, **21**, 271.

190. A. Hara, M. Megata, and S. Yazu: 'Proc. 8th X-ray symp.'; 1969, Kyoto, Japan Society of Materials.

191. A. Hara, M. Megata, and S. Yazu: *Powder Metall. Int.*, 1970, **2**, 43.

192. S. Amberg: *Jernkontorets Ann.*, 1963, **147**, 218.

193. H. W. Newkirk and H. H. Sisler: *J. Am. Ceram. Soc.*, 1958, **41**, 93.

194. J. Graham: *ibid.*, 1959, **42**, 306.

195. H. E. Exner: *Trans. AIME*, 1969, **245**, 677.

196. D. N. French: unpublished work, Ingersoll Rand Research Center, Princeton, NJ

197. B. O. Jaensson: *Mater. Sci. Eng.*, 1971, **8**, 41.

198. H. E. Exner: *J. Mater.*, 1970, 5, (1), 75.

199. V. A. Ivensen, V. A. Chistyakova, and O. N. Eiduk: *Sov. Powder Metall. Met. Ceram.*, 1978, 312.

200. H. Suzuki and K. Hayashi: *Planseeber. Pulvermetall.*, 1977, **25**, 13.

201. I. Kraus: *Czech. J. Phys. B*, 1965, **15**, 367; 1967, **17**, 249.

202. J. Gurland and P. Bardzil: *Trans. AIME*, 1955, **203**, 311.

203. J. Gurland: *ibid.*, 1959, **215**, 601.

204. H. E. Exner and H. F. Fischmeister: *Prakt. Metallogr.*, 1967, **3**, 18.

205. R. Warren: *Planseeber. Pulvermetall.*, 1972, **20**, 299.

206. W. Mader and K. F. Müller: 'Proc. 2nd European symp. for powder metallurgy', Vol. 2, Paper 7. 11; 1968, Stuttgart, Ausschuß für Pulvermetallurgie.

207. W. Mader and K. F. Müller: *Pract. Metallogr.*, 1968, **5**, 616.

208. M. Coster: PhD thesis, Université de Caen, 1974.

209. J. L. Chermant, M. Coster, and A. Deschanvres: *Metallography*, 1975, **8**, 271.

210. K. G. Stjernberg: *Powder Metall.*, 1970, **13**, 1.

211. H. E. Exner: *ibid.*, 429.

212. J. Gurland: *Trans. AIME*, 1963, **227**, 1146.

213. H. F. Fischmeister and H. E. Exner: *Arch. Eisenhüttenwes.*, 1966, **37**, 499.

214. H. Grewe and P. Walter: *Metall*, 1971, **25**, 769.

215. H. Suzuki and T. Tanase: *Planseeber. Pulvermetall.*, 1976, **24**, 271.

216. J. L. Chermant, A. Deschanvres, and F. Osterstock: *Powder Metall.*, 1977, **20**, 63.

217. J. L. Chermant, A. Deschanvres, and F. Osterstock: 'Proc. 4th int. conf. on strength of metals and alloys', Vol. 2, 514; 1976, Nancy.

218. A. Merz, W. Pompe, and G. Grille: 'Proc. 4th European symp. for powder metallurgy', Vol. 2, Paper 5. 8; 1975, Grenoble, Société Française de Métallurgie.

219. H. Suzuki, K. Hayashi, and Terada: unpublished work, 1971, cited in Ref. 181.

220. H. E. Exner, E. Santa Marta, and G. Petzow: 'Modern developments in powder metallurgy', Vol. 4, (ed. H. H. Hausner), 315; 1971, New York, Plenum Press.

221. H. E. Exner and H. Fischmeister: *Z. Metallkd.*, 1966, **57**, 187.

222. H. E. Exner: *ibid.*, 1973, **64**, 273.

223. H. E. Exner: *Int. Metall. Rev.*, 1972, **17**, 25.

224. T. W. Buttler: *Metallography*, 1969, **2**, 289

225. J. Gurland: *Jernkontorets Ann.*, 1963, **147**, 4.

226. T. J. Whalen and M. Humenik: *Trans. AIME*, 1960, **218**, 401.

227. H. Blumenthal and R. Silverman: *ibid.*, 1955, **203**, 1278.

228. R. Kieffer: personal communication, 1978.

229. S. Amberg and H. Doxner: *Powder Metall.*, 1977, **19**, 1.

230. S. Amberg, E. A. Nylander, and B. Uhrenius: *Powder Metall. Int.*, 1974, **6**, 178.

231. H. Suzuki, K. Hayashi, T. Yamamoto, and K. Miyake: *J. Jpn Soc. Powder Metall.*, 1974, 475, **21**, 108, 222.

232. E. Lardner: *Powder Metall.*, 1975, **18**, 47.

233. H. Grewe and G. Osterman: *Tech. Mitt. Krupp*, 1977, **35**, 51.

234. E. A. Almond and B. Roebuck: *Met. Sci.*, 1977, **11**, 458.

235. U. Engel and H. Hübner: *J. Mater. Sci.*, 1978, **13**, (9), 2003.

236. G. A. Wood: *Powder Metall.*, 1970, **13**, 338.

Book review

Binary and multicomponent copper-based systems,
M. E. Drita, N. R. Bochvar, L. S. Guzei, E. V. Lysova,
E. M. Padezhnova, L. L. Rokhlin, and N. I. Turkina,
(ed. N. Kh. Abrikosov), 248 pp, 292 figs., 1979,
Moscow, Nauka, **2 roubles 40 kopeks**

This is a pro-Russian review. Not many Western
scientists realize that one third of the original
work on alloy constitution is carried out in the
USSR and this proportion has been maintained for
the last quarter of a century. Since 1956 the
Russians have meticulously produced annual
volumes under the editorship of the doyen of
Russian metallurgy, Academician N. V. Ageev,
which summarize the work on alloy phase equili-
bria for binary and multicomponent systems
published each year in the world literature. This
series, 'Phase diagrams of metallic systems',
has now reached volume 22, issued in 1978, which
deals with the literature published in 1976.
Throughout the series Academician N. V. Ageev
has been the responsible editor. One may criticize
the details of the presentation of data in this
series but the truth is that there is no comparable
Western publication. All metallurgists admired
the American efforts in publishing critical reviews
of binary alloy systems but regretted the end of
the series with the publication of the book by
F. Shunk in 1969*. The Russian annual volumes,
although not critical, have covered the gap left by
the subsidence of the American effort in the past
decade. More important, they have provided the
only reference to world literature on ternary and
more complex systems. The Russian annual
volumes march on and the world scientific com-
munity must hope that this state of affairs will
continue for many years to come.

With the publication of the present volume we
are now further in the Russians' debt. This volume
is a reference book for all interested in the con-
stitution of copper-base alloys. It contains a sec-
tion reviewing binary systems, a section devoted
to ternary systems, and a final section incorporat-
ing our knowledge of quaternary and quinary
systems. Three appendixes deal with chemical
etchants for copper alloys, the electrolytic etching
of copper alloys, and the physico-chemical proper-
ties of the elements. Finally, 21 references are
given to major works on the physico-chemical
analysis of copper-base alloys.

The authors, all with established reputations
for their original work in the alloy phase equilib-
rium field, make it clear in the preface that they
have reviewed the literature up to 1977. They pay
greater attention to alloy systems of industrial
significance although they claim to review all

known systems. The section concerned with binary
systems contains reviews of 71 systems. It is
interesting to note that we have no data for copper
systems with K, Rb, Cs, and Tc and that, apart from
Th, Pu, and U, we are ignorant of the reactions of
copper with other actinides. It is relatively easy
for a reviewer to pick up specific deficiencies and
to appear erudite while failing to acknowledge the
impact of the broad sweep of the work. The present
reviewer has had the privilege of corresponding
with Professor Y. Austin Chang of the University
of Wisconsin, Milwaukee, who has been concerned
over the past few years to produce critical re-
views of ternary copper-base systems under the
sponsorship of the International Copper Research
Association. The first fruits of Chang's labours
was published in *J. Physical and Chemical Refer-
ence Data*, 1977, **6**, (3), 621–673. In this paper a
re-evaulation of the binary Cu–Fe system is given,
based on the sorting out of a muddle in the litera-
ture on the conversion between atomic and weight
percentages. Readers of the Russian book under
review may with to consult pages 633–635 of
Chang's paper before accepting the data on the
Cu–Fe system

The major importance of the present publica-
tion is in the reviewing of all the scattered litera-
ture on ternary and more complex copper-base
systems. Some 243 ternary systems are included,
together with 39 quaternary systems and 2 quinary
systems. As the authors state in their preface,
space limitations have dictated relatively brief
descriptions of individual systems but more
weight is attached to commercially important
alloys as was the case for binary systems. Any
reader requiring more detail is referred to the
bibliography given for each system. The Western
reader will find some difficulty in finding his way
about this reference book. The authors decided
to arrange the alloy systems in a sequence follow-
ing the Russian alphabet. This is fine if the reader
appreciates the Cyrillic form but a little disturb-
ing to others who find that the binary systems begin
with Cu–N on page 7 whereas we would expect
Cu–Ag on page 51 to head the list. The annual
phase diagram series edited by Academician N. V.
Ageev arranges alloy systems in accordance with
the accepted chemical nomenclature for the ele-
ments so why did we not have a thought spared
for the non-Russian reader in this case?

It is interesting to compare the treatment of
a limited number of ternary copper-base systems
by Chang with the more comprehensive Russian
reference book. Chang has published reviews of 20
ternary systems whereas the present volume con-
tains twelve times the number of ternary systems.
It is not surprising to find that Chang provides
more details on individual systems. What is sur-
prising are the omissions from the Russian book.
No review is included of the Cu–Ag–Pb system

---

*F. A. Shunk: 'Constitution of binary alloys, 2nd
 supplement'; 1969, New York, London, McGraw-
 Hill.

and important references are cited by Chang for the Cu—Ag—Pd, S, Se, and Te systems that are missing from the Russian work. Chang also warns the reader when the results of recent work on binary systems do not agree with older data on ternary systems. The Cu—Ag—Au system is a case in point since the older ternary liquidus data do not agree with the accepted liquidus for the Cu—Au binary system.

No reference work can hope to be absolutely comprehensive. There are data on the existence and crystal structure of ternary intermetallic compounds of copper that are not included in the Russian text. No doubt the second edition will expand the text and fill some of these gaps. In the meantime this volume will be regarded as essential to all concerned with the study and use of copper alloys. One should congratulate our Russian colleagues for the effort they put into the physico-chemical analysis of alloy systems and to ensuring that the data are not left buried in the scientific literature.

A. PRINCE

Pfeil Medal and Prize

The Metals Society's Pfeil Medal and Prize for 1979 has been awarded to Dr F. B. Pickering for his review 'Physical metallurgy of stainless steel developments', *International Metals Reviews,* 1976, **21**, 227—268.

INTERNATIONAL METALS REVIEWS
COMMITTEES IN UK AND USA

MULTICOMPONENT ALLOY CONSTITUTION BIBLIOGRAPHY 1955–1973

by A. Prince

A knowledge of phase equilibria is basic to all interested in materials whether they be metallurgists, materials scientists, ceramicists, geologists, chemists, physicists, or engineers. The relation between the constitution, the microstructure as affected by the constitution, and the material properties as reflected by the microstructure, is of paramount importance to the understanding of materials, to the development of new materials, and to the improvement of existing materials.

The literature on alloy constitution is a rich one. To tap these riches requires that the literature be known and readily available. The purpose of this compilation is to provide a bibliography of references to published work on the constitution of multicomponent systems as a sequel to the references published in Monograph No. 2 of The Institute of Metals, London ('The constitutional diagrams of alloys: a bibliography', J. L. Haughton and A. Prince, 1956, pp. 230–324). The current compilation contains references to work published from January 1955 to December 1973. For the year 1955 only references additional to those included in The Institute of Metals Monograph have been incorporated.

The current compilation contains over 18000 references. References have been given for alloy systems, systems containing metalloids, sulphide systems, and oxide systems where equilibrium with a metal is dealt with. In general, references to equilibria between oxides have not been included. References to crystal structure determinations have been included in addition to publications on phase equilibria. The inorganic synthesis of ternary compounds has been included as have references to work on property–composition relations that provide constitutional data. The growing interest in the calculation of phase equilibria has been recognized by the inclusion of such work.